UNDERSTANDING THE EFFECT OF INTERVENTIONS ON TRANSMISSION DYNAMICS OF EMERGING DISEASES: A CASE STUDY OF COVID-19 PANDEMIC

MEHREEN TARIQ

A THESIS SUBMITTED TO THE FACULTY OF GRADUATE STUDIES
IN PARTIAL FULFILMENT OF THE REQUIREMENTS
FOR THE DEGREE OF
MASTERS OF SCIENCE

GRADUATE PROGRAM IN MATHEMATICS AND STATISTICS
YORK UNIVERSITY
TORONTO, ONTARIO

FEBRUARY 2021

Abstract

Many countries implemented strict social distancing measures to reduce infections, hospitalizations, and deaths during the coronavirus disease 2019 (COVID-19) pandemic. We developed an age-structured deterministic compartmental model and parameterized it with recent COVID-19 estimates to evaluate the effect of self-isolation and stay-at-home orders on infections, hospitalizations, and deaths. The findings show that a 5-month stay-at-home order targeting older individuals (≥ 50 years) had the greatest reduction in hospitalizations (over 47%) and deaths (over 55%). A 5-month stay-at-home order for individuals ≥ 65 years had the most hospitalizations (over 0.0087) and deaths (0.0027) averted per-person practising the stay-at-home order. School closures reduced the outcomes of interest if implemented for a longer duration. Due to the increase in infections post-lockdown (shown in scenario 2), the strategies tested in this study can be used to strategically lift lockdown orders and minimize the burden on healthcare systems until herd immunity is achieved (through vaccination).

Dedication

To my parents, Tariq and Shabana,
to my little brothers, Sarosh and Mobeen,
and to my best friend, Talha;
you are all my stable equilibrium.

Acknowledgements

I would like to start by thanking Allah for all the wonderful opportunities and blessings in my life.

I would like to thank my supervisor, Professor Seyed M. Moghadas, for introducing me to different mathematical modelling techniques, helping me improve my coding skills, and guiding me throughout my thesis work. I greatly appreciate his feedback and comments about optimizing the code, improving the research work, and presentation of the results and figures. Working under his supervision in the ABM-Lab has been a great learning opportunity.

I would like to thank my parents and brothers, Sarosh and Mobeen, for their support and encouragement throughout my academic career. I am extremely grateful to my parents for being so caring and motivating me to achieve my academic and personal goals. I would like to thank my brothers for being my best friends and helping me find the perfect balance between my personal life and research/course work.

I would like to thank my dear friend Ellie Abdollahi for always offering a helping hand throughout my MSc studies. I enjoy our long discussions on math and fashion.

I would like to thank my supervisory committee members, Professor Jude D. Kong and Professor Xin Gao, for their feedback and comments about my research work.

Finally, I would like to thank Talha for motivating me during the final stages of my thesis work. Thank you for listening and being by my side always.

Table of Contents

List of Tables

List of Figures

Chapter 1

Introduction

1.1 Modelling infectious diseases

Despite state of the art pharmaceutical technologies and advances in disease control measures, emerging diseases still inflict substantial morbidity, mortality, and socioeconomic upheavals worldwide. Often, the unpredictable nature of the etiologic agent of the novel pathogen poses significant challenges for all nations to protect the populations at risk. Without any public health interventions, novel diseases may lead to catastrophic outcomes, such as economic woes, societal disruption, long-term illnesses and sequelae, hospitalizations, deaths, and a strain on the healthcare systems. In times of such crisis, preventing these devastating outcomes is a major public health priority which places great pressure on public health professionals and decision-makers to respond rapidly under substantial uncertainty while relying on the best available information. However, this is challenging as there is limited knowledge about the emerging disease during the initial stages of the outbreak. Specifically, there is significant uncertainty regarding the optimality and outcomes of the decisions. This uncertainty is further compounded by the increasingly complex mobility and interaction patterns of modern civilization. The ease of global travel in the modern world combined with the emergence of a highly contagious virus can cause many unwanted illnesses, hospitalizations, and deaths. Although it is difficult to prevent the emergence of novel infectious agents, the existence of powerful tools for generating knowledge, including mathematical and

computational modelling, can help mitigate the impact of emerging diseases and minimize health burden.

Mathematical modelling and simulation methods provide useful and inexpensive decision support tools to generate new knowledge, especially for infectious diseases[1–3]. These tools are widely used to investigate the uncertainties about complex real-world phenomena and provide information about their underlying mechanisms. In the context of emerging infectious diseases, modelling and simulation methods can be useful in exploring different disease characteristics (i.e., reproduction number, transmission probability, disease burden) and projecting the possible outcomes of public health decisions along with their impact on disease spread. Modelling predictions about the potential course of the disease allow public health professionals to make informed decisions and prepare for all possible outcomes, including the unintended consequences of suboptimal interventions.

1.2 The novel coronavirus disease 2019 (COVID-19)

In December 2019, a novel coronavirus SARS-CoV-2 emerged in Wuhan, China [4]. Within days of its initial detection, the virus spread rapidly to many countries, causing the most devastating pandemic in modern times [4]. Individuals from all age-groups and ethnic descents were susceptible to this novel disease, with symptoms ranging from mild to severe [5]. As new information emerged, data suggested that older adults and individuals with underlying medical conditions were at an increased risk for adverse clinical outcomes [6].

The toll of COVID-19 varies across different populations, but has caused many infections, hospitalizations, and deaths worldwide. For countries experiencing severe outbreaks, there is a significant burden on the healthcare system to manage the incoming number of patients, often exceeding the healthcare system capacity[7]. To control the rapid spread of COVID-19 and limit the burden on healthcare systems, most affected countries have resorted to traditional methods (i.e. social distancing policies, stay-at-home orders) as immediate control measures to reduce the daily interactions between individuals in the society. Many countries, including Canada, implemented nation-wide stay-at-home orders, referred to as lockdown, cancelled non-essential travel and closed non-essential

businesses and activities [8]. A news article reported that over 50% of the global population was requested or placed under some type of social distancing order (e.g., curfew, lockdown, and/or school closure) due to the pandemic by April 2020 [9].

1.3 Motivation for research and objectives

Modelling outcomes have played an important role in guiding pandemic response and implementation of control measures during COVID-19 outbreaks. Early findings suggested that without social distancing measures, the disease would be catastrophic; with a rapid and high rise to peak of disease incidence, surge of cases would demand hospitals to manage the incoming number of patients, and many COVID-19 related deaths. Therefore, these social distancing measures became a crucial step to flatten the outbreak curve and reduce the daily number of infections, hospitalizations, and deaths caused by COVID-19. However, optimizing the implementation of these measure at the early stages of COVID-19 may not have been the primary objective of disease control in the midst of a rapidly spreading disease. As of June 2020, there were very limited studies that evaluated the optimality of stay-at-home orders and potential outcomes. This thesis aims to address this knowledge gap and determine the optimal scenarios per capita under which the maximum reduction of disease burden (in terms of total infections, hospitalizations, and deaths) can be achieved.

In this thesis, I propose to evaluate and analyze the impact of stay-at-home orders and self-isolation measures on disease dynamics, with COVID-19 as a case study. Specifically, using recent estimates of COVID-19 characteristics [10], I will determine the effect of these measures and identify which age-groups are most affected under any specific intervention. Understanding the impact of these non-pharmaceutical interventions will provide important information to public health professionals about potential control measures that can be used to minimize burden on healthcare systems and effectively reduce disease spread.

Chapter 2

Background

2.1 Timelines of COVID-19 pandemic events

On December 31, 2019, a cluster of pneumonia cases were reported in the city of Wuhan in the province of Hubei, China [4]. In the subsequent days, health authorities confirmed that these pneumonia cases were caused by a novel coronavirus [4], with symptoms including fever, dry cough, pneumonia, and sometime leading to respiratory failure [11]. At this time, there was not enough information, such as evidence for human-to-human transmission, about the disease to implement important travel restrictions [4]. As a result, infected individuals were able to travel outside of Wuhan, China, without adequate screening or restrictions [12]. By January 16, 2020, the first cases of this novel coronavirus were reported in neighboring countries, including Thailand, South Korea and Japan [4, 11]. Evidence for human-to-human transmission was not announced by health officials until January 19 [4], and this time period between the confirmation of index cases and identification of the main transmission route combined with global travel patterns (i.e., around 30,000 people leave the city of Wuhan everyday [13]) created a window of opportunity for the virus to establish itself with global spread. By January 23, the alarming increase in disease incidence and deaths led to strict quarantine orders and travel restrictions for citizens of Wuhan, that is the home to around 11 million people [11, 13].

Within one month since the first cases were reported, The World Health Organization (WHO) declared an international public health emergency as over 9000 cases of the novel coronavirus were reported in 19 countries around the world [4, 11]. On February 11, 2020, the disease was named COVID-19 (Coronavirus Disease 2019) [4]. In the subsequent days, Italy became one of the "worst hit" countries in Europe, and to control the rising number of COVID-19 cases, government officials enacted lockdown in the northern region and quarantined 16 million people by March 8,2020 [7, 11].

On March 11, WHO confirmed that "COVID-19 could be characterized as a pandemic" [4] . By April 2020, this pandemic had left no alternatives but to enforce lockdown orders and travel restrictions in over 100 countries [11, 14]. By September 2020, more than 27.5 million cases and over 900,000 deaths were reported for COVID-19 [15]. From mid-June to August 2020, many countries implemented re-opening plans, risking the surge of cases and potential for a second wave of the pandemic as lockdown orders were lifted [16]. In many countries, the re-opening phases were associated with enhancing other control measures, such as frequent screening and testing, contact tracing to identify infected individuals, and use of face masks that limit disease spread in the population. The risk of a second peak arose as interactions increased towards normal functioning and movements in the population, and some countries (i.e., the United States) experienced a second and more devastating wave of the COVID-19 with continual rising of cases in Fall 2020 [16, 17].

2.2 Overview of timelines for COVID-19 in Canada

In Canada, the first confirmed case of COVID-19 was reported on January 27, 2020 in a man who returned from Wuhan, China prior to the city's lockdown [8]. In March, a number of cases started to appear throughout the country, including the first community case and COVID-19 related death reported in British Columbia [18]. By March 16, 2020 Canada closed the border for individuals who were not Canadian citizens or permanent residents, with some exceptions, and urged Canadians to avoid non-essential travel [18]. The following day, 4 provinces, including Ontario declared a

state of emergency, banned large gatherings, and closed places such as, community centres, schools, libraries, and theatres [18]. By March 23, 2020 the Public Health Agency of Canada confirmed that community spread was responsible for around 50% of the COVID-19 cases, and thereby highlighting the need for strict stay-at-home orders to control disease spread [18]. From mid-June to July 2020, after the decline of the first pandemic wave, provinces in Canada begun to ease restrictions and progress through the different stages of re-opening plans. Due to the unpredictable nature of SARS-CoV-2, there was still significant uncertainty regarding the timing and extent of the second peak as restrictions were lifted. Acting vigilantly, provinces also prepared for possible surge in COVID-19 cases in Fall 2020.

On September 28, 2020, the province of Ontario recorded 700 new COVID-19 cases, which surpassed the previous high of 640 cases in April, 2020 [19]. At the time, modelling projections suggested the second wave peak incidence to occur in mid to late October for Ontario [19]. During the initial stages of the second wave, majority of the COVID-19 cases were reported in individuals under 40 years of age. Even though these age-groups reported fewer hospitalizations compared to older age-groups, there was a risk of younger age-groups spreading the infection to older and at-risk individuals [19]. Therefore, many health officials recommended a return to Stage 2 [19]. On October 25, the province of Ontario reported its highest daily incidence since the emergence of the virus, which was 1042 cases [20]. The highest number of non-ICU and ICU hospitalizations reported in a single day in Ontario were 1043 cases and 264 cases respectively, during the first wave [19, 20]. In Ontario, as the most populated province in Canada, there are approximately 2000 intensive care unit (ICU) beds, of which about 60% are generally occupied by non-COVID-19 related causes [19]. Researchers estimated that 475 beds are available for non-emergency surgeries and COVID-19 cases combined, and about only 100 of these beds are available for COVID-19 cases when surgeries are performed as scheduled [19], posing a significant strain on hospital capacity to manage COVID-19 patients.

In Canada, a number of provinces, including Ontario, Quebec, and Alberta, released their modelling

outcomes for the pandemic trajectory, which suggested the outbreak could last between 18 months to 2 years [18]. For Ontario, modelling results suggested that over 100,000 COVID-19 related deaths could have occurred in the absence of any control measures; however, with control measures, this estimate reduced to around 3,000 to 15,000 COVID-19 related deaths[18]. Understanding the optimality of different stay-at-home orders will provide valuable insight on future management of COVID-19 and provide critical information about strategies that not only are effective, but also efficient at controlling disease spread.

2.3 Natural history of COVID-19

Clinical and epidemiological studies of COVID-19 indicate that the course of disease includes two distinct pathways of asymptomatic and symptomatic infection [21]. During asymptomatic infection, individuals present no symptoms of the disease, become infectious after the (non-infectious) latent period, and can transmit the disease during their infectious period. Identification of asymptomatic cases using symptom-based screening is impractical, and requires laboratory testing. In the symptomatic pathway, infected individuals proceed to a highly infectious stage of pre-symptomatic infection after the latent period. The onset of symptoms in these individuals will mark the end of the incubation period. Infected cases who experience the symptomatic path are able to transmit the disease during both pre-symptomatic stage and the remaining duration of their infectious period after the onset of symptoms (2.1). Recent study suggest that the peak of infectiousness in symptomatic cases occur -0.9 (i.e. pre-symptomatic stage) to 0.9 days from the onset of symptoms [22], indicating the potential for significant disease transmission during the incubation period in the pre-symptomatic stage [23]. Since asymptomatic and pre-symptomatic cases do not display any symptoms, they are referred to as the ‘silent infection’.

The duration of incubation period varies among COVID-19 cases before developing symptoms. Early estimates were consistent on the incubation period having a lognormal distribution with an average of 5.2 days [10, 24]. A recent study, using a statistical method for addressing the

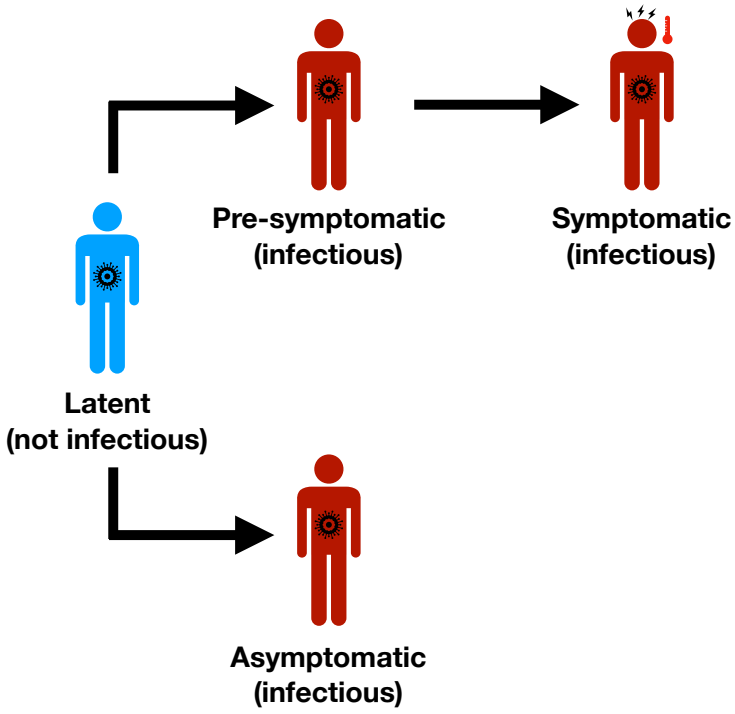

Figure 2.1: Latent and infectious stages of COVID-19.

recall-bias, shows that the incubation period can be as long as 8.29 days on average [25]. The start of infectiousness during the incubation period marks the beginning of the course of disease in which transmission can occur. The onset of infectiousness varies in infected individuals and could be as long as 12.3 days on average before symptom onset, but for most cases it occurs 5 to 6 days prior to symptom onset [22]. This time period corresponds to the pre-symptomatic stage. It is estimated that the peak of infectiousness may occur 1 day before to 1 day after start of symptomatic stage [22]. After the peak, infectiousness declines monotonically over the course of symptomatic disease while symptoms are resolved. [22].

Silent transmission is a major contributor to the overall COVID-19 disease transmission [23, 26, 27]. The COVID-19 outbreak on Diamond Princess cruise ship found that 17.9% of individuals were asymptomatic [26], while another study estimated the asymptomatic proportion of cases to be 30.8% [27]. A modelling study investigated the impact of silent infections on disease spread and

concluded that during an outbreak, transmission from asymptomatic and pre-symptomatic cases may account for over 50% of the total incidence (i.e., the overall attack rate of an outbreak) [23]. The study further explains that even with immediate self-isolation of symptomatic individuals, this level of transmission would be sufficient to sustain the outbreak [23]. The study findings indicate that for 17.9% and 30.8% of asymptomatic proportions estimated in previous studies, 48% and 47% of transmission were caused during the pre-symptomatic stage, respectively [23] . The corresponding transmission rates by asymptomatic infections were estimated to be 3.4% and 6.6%, respectively [23]. Given these findings, bringing the attack rate to below 1% would require screening protocols that can detect at least 33% of silent infections [23].

Individuals with symptomatic disease (presenting symptoms such as fever, cough, sneeze) may recover without the need for hospitalization. However, severe symptoms may occur (e.g., difficulty in breathing), which may require hospitalization, and in some cases with critical condition, may necessitate the use of intensive care and ventilator [5]. A modelling study in the context of the United States population projected the number of intensive care unit (ICU) beds that would be required during the peak of the COVID-19 outbreak to be 3.8 times more than the total available ICU beds if interventions such as self-isolation of mildly symptomatic cases were at low rates (< 20%) [28]. Strikingly, even with the self-isolation of 20% of symptomatic individuals within 24 hours of symptom onset, the projected number of required ICU beds still exceeded the existing number of ICU beds in United States [28]. Their results highlighted the impact of COVID-19 on the healthcare systems along with the need to expand the critical care capacity for disease management [28, 29].

Chapter 3

COVID-19 Modelling Framework

This chapter outlines the methods used in this research work. A detailed description of the compartmental model is provided in section 3.1, and the model assumptions are listed in section 3.2. This research work uses an age-structured Susceptible-Exposed-Infected-Recovered (SEIR) modelling framework to model the transmission dynamics of COVID-19. Based on major modelling outcomes on COVID-19 [23, 28, 30], the model was extended to incorporate compartments of hospitalization, silent infections, and self-isolation, with the inclusion of stay-at-home strategies in different age groups. Section 3.3 shows the next generation method which is a widely used approach to theoretically calculate the reproduction number ($\mathcal{R}_0$).

3.1 Model description

The description of each model compartment is given in Table 3.1. The population was divided into five age-groups: $0-4$, $5-19$, $20-49$, $50-64$, and $65+$ years. With this age-structure, age-specific control strategies can be tested in this modelling work. The community and household contact rates between individuals in age-group a and age-group c are denoted by $M_{a,c}$ and $\tilde{M}_{a,c}$, respectively. Figure 3.1 shows the schematic diagram of the model structure.

For simplicity, let $S_a x$ and $S_a y$ represent the community transmission and household transmission (infection transmission by infected individuals in self-isolation) between susceptible and infectious

Variable	Description
S_a	Susceptible individuals in age group a
E_a	Exposed and latent individuals in age group a
A_a	Asymptomatic individuals in age group a
$P_{m,a}$	Pre-symptomatic cases who will develop mild symptoms in age group a
$I_{m,a}$	Symptomatic mild cases in age group a
$Q_{m,a}$	Symptomatic mild cases who practise self-isolation in age group a
$P_{s,a}$	Pre-symptomatic cases who will develop severe symptoms in age group a
$I_{s,a}$	Symptomatic severe cases in age group a
$Q_{s,a}$	Symptomatic severe cases who practise self-isolation in age group a
H_a	Hospitalized individuals for age group a
C_a	Individuals admitted to ICU for age group a
R_a	Recovering individuals for age group a
D_a	Infected individuals who died for age group a
N_a	Population size for age group a
$M_{a,c}$	Community contact rate between individuals in age group a and individuals in age group c
$\tilde{M}_{a,c}$	Household contact rate between individuals in age group a and individuals in age group c

Table 3.1: Description of important model variables

individuals, where

$$x = \beta \sum_{j=1}^{5} M_{a,j} \frac{(P_{m,j} + P_{s,j} + \kappa_m I_{m,j} + \kappa_s I_{s,j} + \alpha A_j)}{N_j},$$
$$y = \beta \sum_{j=1}^{5} \tilde{M}_{a,j} \frac{(\kappa_m Q_{m,j} + \kappa_s Q_{s,j})}{N_j}.$$

3.1.1 Susceptible and exposed individuals

Individuals in S_a are susceptible to COVID-19. Upon infection, individuals move from the susceptible class (S_a) of age-group a to the exposed class (E_a) of age-group a. Infected individuals in the exposed class (E_a) become infectious after an average latent period of $1/\sigma$ days. These dynamics are described by the equations:

$$\frac{\mathrm{d}S_a}{\mathrm{d}t} = -S_a x - S_a y,$$
$$\frac{\mathrm{d}E_a}{\mathrm{d}t} = S_a x + S_a y - \sigma E_a.$$

3.1.2 Asymptomatic individuals

A proportion p_a of infectious individuals enter the asymptomatic class (A_a) presenting no symptoms. These individuals remain infectious for an average duration of $1/\eta$ days and recover at the end of their infectious period, as described by

$$\frac{\mathrm{d}A_a}{\mathrm{d}t} = p_a \sigma E_a - \eta A_a$$

3.1.3 Pre-symptomatic, symptomatic, and self-isolated individuals with mild illness

A proportion $(1-p_a)q_a$ of highly infectious individuals enter the pre-symptomatic class ($P_{m,a}$) after the latent period. These individuals do not show any symptoms for an average pre-symptomatic period of $1/\theta$ days, after which they enter the symptomatic stage ($I_{m,a}$) with mild illness. These cases remain infectious for an average period of $1/\gamma$ days before recovery. We assume that a proportion f_a of mildly symptomatic individuals self-isolate within $1/\tau$ days of symptom onset and enter the self-isolation class ($Q_{m,a}$). Self-isolated individuals will recover after an average infectious period of $(\tau-\gamma)/\tau\gamma$.The remaining proportion $(1-f_a)$ of symptomatic individuals will be infectious for $1/\gamma$ days until recovery. These dynamics are described by

$$\begin{aligned}
\frac{\mathrm{d}P_{m,a}}{\mathrm{d}t} &= (1-p_a)q_a\sigma E_a - \theta P_{m,a} \\
\frac{\mathrm{d}I_{m,a}}{\mathrm{d}t} &= \theta P_{m,a} - (1-f_a)\gamma I_{m,a} - f_a \tau I_{m,a} \\
\frac{\mathrm{d}Q_{m,a}}{\mathrm{d}t} &= f_a \tau I_{m,a} - \gamma \left(\frac{\tau}{\tau-\gamma}\right) Q_{m,a}
\end{aligned}$$

3.1.4 Pre-symptomatic, symptomatic, and self-isolated individuals with severe illness

A proportion $(1-p_a)(1-q_a)$ of highly infectious individuals enter the pre-symptomatic class for severe illness ($P_{s,a}$) after the latent period. These individuals do not show any symptoms for an average pre-symptomatic period of $1/\theta$ days, after which they enter the symptomatic class ($I_{s,a}$). A proportion g_a of individuals exhibiting severe symptoms self-isolate and enter the class ($Q_{s,a}$) until their recovery. The infectious period for these individuals from the start of isolation is $(\tau-\gamma)/\tau\gamma$. We assumed that a proportion h_a of severely ill individuals will require hospitalization after $1/\delta$ days following symptom onset. The remaining proportion $(1-g_a-h_a)$ of severe cases will be infectious for $1/\gamma$ days until recovery without hospitalization. These dynamics are described by:

$$\begin{aligned}
\frac{\mathrm{d}P_{s,a}}{\mathrm{d}t} &= (1-p_a)(1-q_a)\sigma E_a - \theta P_{s,a} \\
\frac{\mathrm{d}I_{s,a}}{\mathrm{d}t} &= \theta P_{s,a} - (1-g_a-h_a)\gamma I_{s,a} - g_a\tau I_{s,a} - h_a\delta I_{s,a} \\
\frac{\mathrm{d}Q_{s,a}}{\mathrm{d}t} &= g_a\tau I_{s,a} - \gamma\left(\frac{\tau}{\tau-\gamma}\right) Q_{s,a}
\end{aligned}$$

3.1.5 Hospitalized individuals

A proportion h_a of severe symptomatic cases ($I_{s,a}$) require hospitalization. For hospitalized cases, only a fraction c_a of them are admitted to the ICU (C_a) while the remaining fraction $(1-c_a)$ remain hospitalized (H_a) until recovery without ICU admission. Proportions d_a and m_a of non-ICU and ICU cases, respectively, die after $1/\mu$ days. The remaining proportions $(1-d_a)$ and $(1-m_a)$ of hospitalized patients recover after $1/\phi$ days and $1/\psi$ days of non-ICU and ICU hospitalization, respectively. These dynamics are described by:

$$\frac{\mathrm{d}H_a}{\mathrm{d}t} = (1-c_a)h_a\delta I_{s,a} - \left(d_a\mu + (1-d_a)\phi\right) H_a$$

$$\frac{\mathrm{d}C_a}{\mathrm{d}t} = c_a h_a \delta I_{s,a} - (m_a\mu + (1-m_a)\psi)\, C_a$$

3.1.6 Recovered and dead individuals

Infected individuals enter the recovered class (R_a) after the end of their infectious period. Individuals who die during hospitalization enter the dead class (D_a). These dynamics are described by:

$$\begin{aligned}\frac{\mathrm{d}R_a}{\mathrm{d}t} &= \eta A_a + \gamma\left(\frac{\tau}{\tau-\mu}\right)(Q_{s,a}+Q_{m,a}) + (1-d_a)\phi H_a + (1-m_a)\psi C_a \\ &\quad + (1-f_a)\gamma I_{m,a} + (1-g_a-h_a)\gamma I_{s,a} \\ \frac{\mathrm{d}D_a}{\mathrm{d}t} &= d_a\mu H_a + m_a\mu C_a\end{aligned}$$

In summary, the model dynamics (represented by a schematic diagram in Figure 3.1) consists of the following equations for each age-group:

$$\frac{\mathrm{d}S_a}{\mathrm{d}t} = -S_a x - S_a y \tag{3.1}$$
$$\frac{\mathrm{d}E_a}{\mathrm{d}t} = S_a x + S_a y - \sigma E_a \tag{3.2}$$
$$\frac{\mathrm{d}A_a}{\mathrm{d}t} = p_a\sigma E_a - \eta A_a \tag{3.3}$$
$$\frac{\mathrm{d}P_{m,a}}{\mathrm{d}t} = (1-p_a)q_a\sigma E_a - \theta P_{m,a} \tag{3.4}$$
$$\frac{\mathrm{d}I_{m,a}}{\mathrm{d}t} = \theta P_{m,a} - (1-f_a)\gamma I_{m,a} - f_a\tau I_{m,a} \tag{3.5}$$
$$\frac{\mathrm{d}Q_{m,a}}{\mathrm{d}t} = f_a\tau I_{m,a} - \gamma\left(\frac{\tau}{\tau-\gamma}\right)Q_{m,a} \tag{3.6}$$
$$\frac{\mathrm{d}P_{s,a}}{\mathrm{d}t} = (1-p_a)(1-q_a)\sigma E_a - \theta P_{s,a} \tag{3.7}$$
$$\frac{\mathrm{d}I_{s,a}}{\mathrm{d}t} = \theta P_{s,a} - (1-g_a-h_a)\gamma I_{s,a} - g_a\tau I_{s,a} - h_a\delta I_{s,a} \tag{3.8}$$

$$\frac{\mathrm{d}Q_{s,a}}{\mathrm{d}t} = g_a\tau I_{s,a} - \gamma\left(\frac{\tau}{\tau-\gamma}\right)Q_{s,a} \tag{3.9}$$

$$\frac{\mathrm{d}H_a}{\mathrm{d}t} = (1-c_a)h_a\delta I_{s,a} - (d_a\mu + (1-d_a)\phi)\,H_a \tag{3.10}$$

$$\frac{\mathrm{d}C_a}{\mathrm{d}t} = c_a h_a \delta I_{s,a} - (m_a\mu + (1-m_a)\psi)\,C_a \tag{3.11}$$

$$\frac{\mathrm{d}R_a}{\mathrm{d}t} = \eta A_a + \gamma\left(\frac{\tau}{\tau-\mu}\right)(Q_{s,a}+Q_{m,a}) + (1-d_a)\phi H_a + (1-m_a)\psi C_a \tag{3.12}$$
$$+(1-f_a)\gamma I_{m,a} + (1-g_a-h_a)\gamma I_{s,a}$$

$$\frac{\mathrm{d}D_a}{\mathrm{d}t} = d_a\mu H_a + m_a\mu C_a \tag{3.13}$$

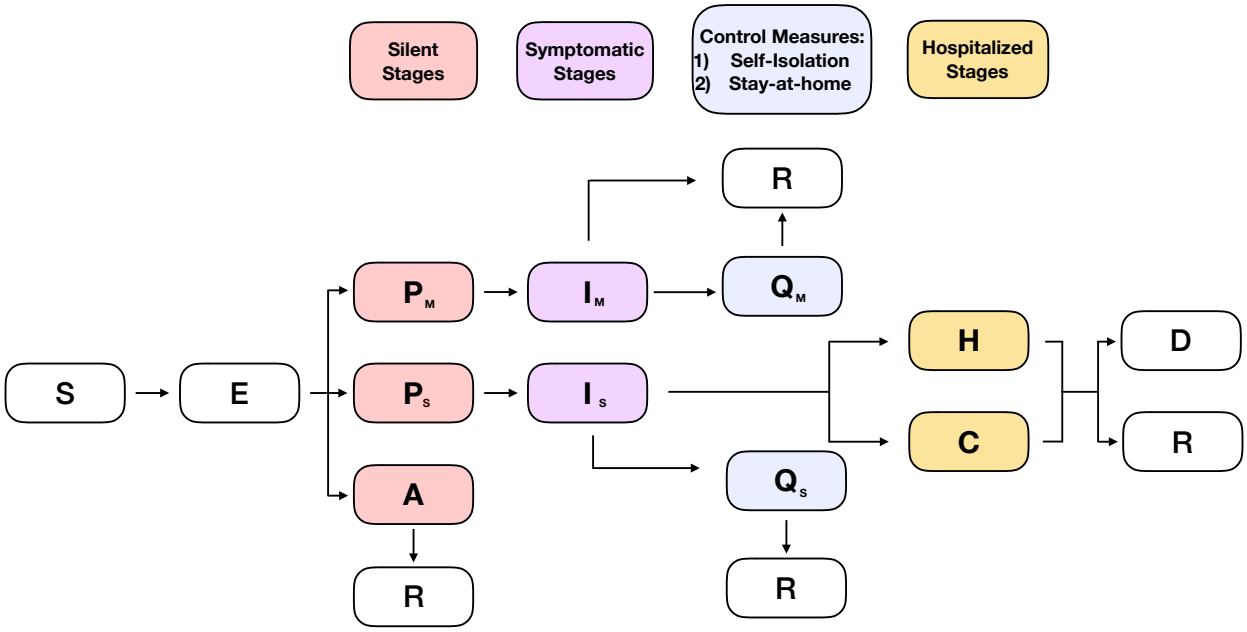

Figure 3.1: A schematic diagram of the model dynamics. There are 13 age-specific compartments in this model that include susceptible (S_a), exposed (E_a), asymptomatic (A_a), pre-symptomatic for mild illness ($P_{m,a}$), pre-symptomatic for severe illness ($P_{s,a}$), symptomatic with mild illness ($I_{m,a}$), symptomatic with severe illness ($I_{s,a}$), self-isolated with mild illness ($Q_{m,a}$), self-isolated with severe illness ($Q_{s,a}$), non-ICU hospitalized (H_a), admitted to ICU (C_a), recovered (R_a), and dead (D_a) classes.

3.2 Model assumptions

Key assumptions made in this modelling framework are listed below:

- Asymptomatic individuals do not self-isolate and do not require hospitalization.
- Mild symptomatic cases do not require hospitalization.
- Severe cases who do not require hospitalization would self-isolate until recovery.
- Infected individuals who self-isolate remain in isolation until recovery.
- Contact rates of individuals practising stay-at-home order or self-isolation are determined by the household contact matrix.
- Hospitalized individuals do not contribute to disease transmission as they are considered perfectly isolated due to infection control measures in the hospital.
- Disease transmission occurs only through contact between susceptible and infectious individuals (i.e., infection through other modes are not considered in this model).
- Recovered individuals gain adequate immunity and are no longer susceptible to the disease for the duration of simulations.

3.3 Basic reproduction number ($\mathcal{R}_0$)

The basic reproduction number ($\mathcal{R}_0$) is "the number of secondary cases generated by a single infected individual during his or her entire infectious period, in a population which is entirely susceptible" [31]. This important quantity in epidemiology determines whether the epidemic will occur (if $\mathcal{R}_0 > 1$) or die out (if $\mathcal{R}_0 < 1$) in the population [31]. Estimates of this quantity can help determine the possibility of a large outbreak, and identify the type and intensity of interventions required for control or mitigation.

3.3.1 Disease free equilibrium (DFE)

The DFE is a fixed point that represents the state of the population free of infection. For model (3.1)-(3.13), the DFE is given by

$$[S_a, E_a, A_a, P_{m,a}, I_{m,a}, Q_{m,a}, P_{s,a}, I_{s,a}, Q_{s,a}, H_a, C_a, R_a, D_a] = [S_{DFE}, 0, \cdots, 0]$$

where

$$S_{DFE} = [N_1, N_2, N_3, N_4, N_5]$$

and N_a represents the total population of age group a. In order to obtain $\mathcal{R}_0$, we use the next generation method at the DFE as described in the following section.

3.3.2 Next generation matrix (NGM)

To apply the NGM technique, the compartments of model (3.1)-(3.13) were divided into two categories: (i) compartments of infected individuals that do not include any control measure, and (ii) remaining compartments of infected and uninfected individuals. The first category is included in a vector X (30×1 dimension), and the second category is included in a vector Y (35×1 dimension) as expressed by:

$$X = \Big(E_a, A_a, P_{m,a}, I_{m,a}, P_{s,a}, I_{s,a}\Big)$$
$$Y = \Big(S_a, Q_{m,a}, Q_{s,a}, H_a, C_a, R_a, D_a\Big)$$

The equations for X can be written as [32, 33]:

$$\frac{dX_i}{dt} = f_i(x) = \mathcal{F}_i(x) - \mathcal{V}_i(x) \tag{3.14}$$

Here, $\mathcal{F}_i(x)$ represents the new infection rates, while $\mathcal{V}_i(x)$ represents the rates of transfer between classes [32, 33]. We made the assumption that both functions are twice continuously

differentiable for each vector variable [32, 33]. The vector $\mathcal{V}_i(x)$ represents rates of transfer in compartment i: $\mathcal{V}_i(x) = V_i^- - V_i^+$, were V_i^- includes the rates of transfer for individuals leaving the compartment i and V_i^+ represents the rates of transfer for individuals entering the compartment i.

Since we are calculating the basic reproduction number in the absence of any control measures, the parameters associated with self-isolation (f_a and g_a) and hospitalizations (h_a and c_a) were set to zero. For the model (3.1)-(3.13), functions $\mathcal{F}$ and $\mathcal{V}$ are given by:

$$\mathcal{F} = \begin{pmatrix} f_1 \\ \vdots \\ f_5 \\ f_6 \\ \vdots \\ f_{30} \end{pmatrix} = \begin{pmatrix} \beta S_1 \sum_{j=1}^{5} M_{1,j} \frac{(P_{m,j}+P_{s,j}+\kappa_m I_{m,j}+\kappa_s I_{s,j}+\alpha A_j)}{N_j} \\ \vdots \\ \beta S_5 \sum_{j=1}^{5} M_{5,j} \frac{(P_{m,j}+P_{s,j}+\kappa_m I_{m,j}+\kappa_s I_{s,j}+\alpha A_j)}{N_j} \\ 0 \\ \vdots \\ 0 \end{pmatrix}$$

$$\mathcal{V} = \begin{pmatrix} v_1 \\ \vdots \\ v_6 \\ \vdots \\ v_{11} \\ \vdots \\ v_{16} \\ \vdots \\ v_{21} \\ \vdots \\ v_{26} \\ \vdots \\ v_{30} \end{pmatrix} = \begin{pmatrix} \sigma E_1 \\ \vdots \\ -p_1\sigma E_1 + \eta A_1 \\ \vdots \\ -(1-p_1)q_1\sigma E_1 + \theta P_{m,1} \\ \vdots \\ -\theta P_{m,1} + \gamma I_{m,1} \\ \vdots \\ -(1-p_1)(1-q_1)\sigma E_1 + \theta P_{s,1} \\ \vdots \\ -\theta P_{s,1} + \gamma I_{s,1} \\ \vdots \\ -\theta P_{s,5} + \gamma I_{s,5} \end{pmatrix}$$

The $\mathcal{R}_0$ expression can be expressed using Lemma 1 and equation 4 from [32].

Lemma 1 [32]: If x_0 is a DFE (Disease Free Equilibrium) of 3.14 and $f_i(x)$ satisfies (A1) - (A5), then the derivatives $D\mathcal{F}(x_0)$ and $D\mathcal{V}(x_0)$ are partitioned as $D\mathcal{F}(x_0) = \left(\begin{smallmatrix} F & 0 \\ 0 & 0 \end{smallmatrix}\right)$ and $D\mathcal{V}(x_0) = \left(\begin{smallmatrix} V & 0 \\ J_3 & J_4 \end{smallmatrix}\right)$ where F and V are dimension m by m defined by $F = \frac{(D\mathcal{F}_i)}{(dX_j)}(x_0)$ and $V = \frac{(D\mathcal{V}_i)}{(dX_j)}(x_0)$, with $1 \leq i, j \leq m$. Further, F is non-negative, V is a non-singular M-matrix and all eigenvalues of J_4 have positive real parts.

To find matrix F and V, we need to calculate the Jacobian of (3.1)-(3.13) around the DFE:

$$F = \frac{d\mathcal{F}_i(DFE)}{dX_j},$$
$$V = \frac{d\mathcal{V}_i(DFE)}{dX_j}$$

with

$$F = \begin{bmatrix} 0 & A & P & I_m & P & I_s \\ 0 & 0 & 0 & 0 & 0 & 0 \\ 0 & 0 & 0 & 0 & 0 & 0 \\ 0 & 0 & 0 & 0 & 0 & 0 \\ 0 & 0 & 0 & 0 & 0 & 0 \\ 0 & 0 & 0 & 0 & 0 & 0 \end{bmatrix} \tag{3.15}$$

Matrices A, P, I_m, and I_s are described by:

$$A = \begin{bmatrix} \beta\alpha M_{1,1}\frac{N_1}{N_1} & \beta\alpha M_{1,2}\frac{N_1}{N_2} & \beta\alpha M_{1,3}\frac{N_1}{N_3} & \beta\alpha M_{1,4}\frac{N_1}{N_4} & \beta\alpha M_{1,5}\frac{N_1}{N_5} \\ \beta\alpha M_{2,1}\frac{N_2}{N_1} & \beta\alpha M_{2,2}\frac{N_2}{N_2} & \beta\alpha M_{2,3}\frac{N_2}{N_3} & \beta\alpha M_{2,4}\frac{N_2}{N_4} & \beta\alpha M_{2,5}\frac{N_2}{N_5} \\ \beta\alpha M_{3,1}\frac{N_3}{N_1} & \beta\alpha M_{3,2}\frac{N_3}{N_2} & \beta\alpha M_{3,3}\frac{N_3}{N_3} & \beta\alpha M_{3,4}\frac{N_3}{N_4} & \beta\alpha M_{3,5}\frac{N_3}{N_5} \\ \beta\alpha M_{4,1}\frac{N_4}{N_1} & \beta\alpha M_{4,2}\frac{N_4}{N_2} & \beta\alpha M_{4,3}\frac{N_4}{N_3} & \beta\alpha M_{4,4}\frac{N_4}{N_4} & \beta\alpha M_{4,5}\frac{N_4}{N_5} \\ \beta\alpha M_{5,1}\frac{N_5}{N_1} & \beta\alpha M_{5,2}\frac{N_5}{N_2} & \beta\alpha M_{5,3}\frac{N_5}{N_3} & \beta\alpha M_{5,4}\frac{N_5}{N_4} & \beta\alpha M_{5,5}\frac{N_5}{N_5} \end{bmatrix}$$

$$P = \begin{bmatrix} \beta M_{1,1}\frac{N_1}{N_1} & \beta M_{1,2}\frac{N_1}{N_2} & \beta M_{1,3}\frac{N_1}{N_3} & \beta M_{1,4}\frac{N_1}{N_4} & \beta M_{1,5}\frac{N_1}{N_5} \\ \beta M_{2,1}\frac{N_2}{N_1} & \beta M_{2,2}\frac{N_2}{N_2} & \beta M_{2,3}\frac{N_2}{N_3} & \beta M_{2,4}\frac{N_2}{N_4} & \beta M_{2,5}\frac{N_2}{N_5} \\ \beta M_{3,1}\frac{N_3}{N_1} & \beta M_{3,2}\frac{N_3}{N_2} & \beta M_{3,3}\frac{N_3}{N_3} & \beta M_{3,4}\frac{N_3}{N_4} & \beta M_{3,5}\frac{N_3}{N_5} \\ \beta M_{4,1}\frac{N_4}{N_1} & \beta M_{4,2}\frac{N_4}{N_2} & \beta M_{4,3}\frac{N_4}{N_3} & \beta M_{4,4}\frac{N_4}{N_4} & \beta M_{4,5}\frac{N_4}{N_5} \\ \beta M_{5,1}\frac{N_5}{N_1} & \beta M_{5,2}\frac{N_5}{N_2} & \beta M_{5,3}\frac{N_5}{N_3} & \beta M_{5,4}\frac{N_5}{N_4} & \beta M_{5,5}\frac{N_5}{N_5} \end{bmatrix}$$

$$I_m = \begin{bmatrix} \beta\kappa_m M_{1,1}\frac{N_1}{N_1} & \beta\kappa_m M_{1,2}\frac{N_1}{N_2} & \beta\kappa_m M_{1,3}\frac{N_1}{N_3} & \beta\kappa_m M_{1,4}\frac{N_1}{N_4} & \beta\kappa_m M_{1,5}\frac{N_1}{N_5} \\ \beta\kappa_m M_{2,1}\frac{N_2}{N_1} & \beta\kappa_m M_{2,2}\frac{N_2}{N_2} & \beta\kappa_m M_{2,3}\frac{N_2}{N_3} & \beta\kappa_m M_{2,4}\frac{N_2}{N_4} & \beta\kappa_m M_{2,5}\frac{N_2}{N_5} \\ \beta\kappa_m M_{3,1}\frac{N_3}{N_1} & \beta\kappa_m M_{3,2}\frac{N_3}{N_2} & \beta\kappa_m M_{3,3}\frac{N_3}{N_3} & \beta\kappa_m M_{3,4}\frac{N_3}{N_4} & \beta\kappa_m M_{3,5}\frac{N_3}{N_5} \\ \beta\kappa_m M_{4,1}\frac{N_4}{N_1} & \beta\kappa_m M_{4,2}\frac{N_4}{N_2} & \beta\kappa_m M_{4,3}\frac{N_4}{N_3} & \beta\kappa_m M_{4,4}\frac{N_4}{N_4} & \beta\kappa_m M_{4,5}\frac{N_4}{N_5} \\ \beta\kappa_m M_{5,1}\frac{N_5}{N_1} & \beta\kappa_m M_{5,2}\frac{N_5}{N_2} & \beta\kappa_m M_{5,3}\frac{N_5}{N_3} & \beta\kappa_m M_{5,4}\frac{N_5}{N_4} & \beta\kappa_m M_{5,5}\frac{N_5}{N_5} \end{bmatrix}$$

and, for I_s, replace κ_m in I_m with κ_s.

Similarly, V is the matrix:

$$V = \begin{bmatrix} v_1 & 0 & 0 & 0 & 0 & 0 \\ v_2 & v_3 & 0 & 0 & 0 & 0 \\ v_4 & 0 & v_5 & 0 & 0 & 0 \\ 0 & 0 & -v_5 & v_6 & 0 & 0 \\ v_7 & 0 & 0 & 0 & v_5 & 0 \\ 0 & 0 & 0 & 0 & -v_5 & v_6 \end{bmatrix} \tag{3.16}$$

with

$$v_1 = \begin{bmatrix} \sigma & 0 & 0 & 0 & 0 \\ 0 & \sigma & 0 & 0 & 0 \\ 0 & 0 & \sigma & 0 & 0 \\ 0 & 0 & 0 & \sigma & 0 \\ 0 & 0 & 0 & 0 & \sigma \end{bmatrix}.$$

$$v_2 = \begin{bmatrix} -p_1\sigma & 0 & 0 & 0 & 0 \\ 0 & -p_2\sigma & 0 & 0 & 0 \\ 0 & 0 & -p_3\sigma & 0 & 0 \\ 0 & 0 & 0 & -p_4\sigma & 0 \\ 0 & 0 & 0 & 0 & -p_5\sigma \end{bmatrix}.$$

$$v_3 = \begin{bmatrix} \eta & 0 & 0 & 0 & 0 \\ 0 & \eta & 0 & 0 & 0 \\ 0 & 0 & \eta & 0 & 0 \\ 0 & 0 & 0 & \eta & 0 \\ 0 & 0 & 0 & 0 & \eta \end{bmatrix}.$$

$$v_4 = \begin{bmatrix} -\sigma q_1(1-p_1) & 0 & 0 & 0 & 0 \\ 0 & -\sigma q_2(1-p_2) & 0 & 0 & 0 \\ 0 & 0 & -\sigma q_3(1-p_3) & 0 & 0 \\ 0 & 0 & 0 & -\sigma q_4(1-p_4) & 0 \\ 0 & 0 & 0 & 0 & -\sigma q_5(1-p_5) \end{bmatrix}.$$

$$v_5 = \begin{bmatrix} \theta & 0 & 0 & 0 & 0 \\ 0 & \theta & 0 & 0 & 0 \\ 0 & 0 & \theta & 0 & 0 \\ 0 & 0 & 0 & \theta & 0 \\ 0 & 0 & 0 & 0 & \theta \end{bmatrix}.$$

$$v_6 = \begin{bmatrix} \gamma & 0 & 0 & 0 & 0 \\ 0 & \gamma & 0 & 0 & 0 \\ 0 & 0 & \gamma & 0 & 0 \\ 0 & 0 & 0 & \gamma & 0 \\ 0 & 0 & 0 & 0 & \gamma \end{bmatrix}.$$

For simplicity, let $z_a = -\sigma(1-q_a)(1-p_a)$, where $a = 1, 2, 3, 4, 5$. Now using z_a, v_7 is written as:

$$v_7 = \begin{bmatrix} z_1 & 0 & 0 & 0 & 0 \\ 0 & z_2 & 0 & 0 & 0 \\ 0 & 0 & z_3 & 0 & 0 \\ 0 & 0 & 0 & z_4 & 0 \\ 0 & 0 & 0 & 0 & z_5 \end{bmatrix}.$$

Multiplying F and V^{-1}, we obtain the NGM (denoted by G) [32]. "The entries of G give the rate at which infected individuals in X_j produce new infections in X_i, times the average length of time an individual spends in a single visit to compartment j" [31]. The largest eigenvalue in magnitude (i.e., the spectral radius) of G is defined as the basic reproduction number [32]:

$$\mathcal{R}_0 = \rho(FV^{-1}) \tag{3.17}$$

For model (3.1)-(3.13), G is expressed by:

$$G = \begin{bmatrix} K1 & K2 & K3 & K4 & K5 & K6 \\ 0 & 0 & 0 & 0 & 0 & 0 \\ 0 & 0 & 0 & 0 & 0 & 0 \\ 0 & 0 & 0 & 0 & 0 & 0 \\ 0 & 0 & 0 & 0 & 0 & 0 \\ 0 & 0 & 0 & 0 & 0 & 0 \end{bmatrix} \tag{3.18}$$

with

$$K1 = \frac{\beta M(i,j)S_i}{N_j}\left(\frac{\alpha p(j)}{\eta} + \frac{1-p(j)}{\theta} + \frac{(p(j)-1)(\kappa_s(q(j)-1)-\kappa_m q(j))}{\gamma}\right),$$
$$K2 = \frac{\beta\alpha M(i,j)S_i}{N_j\eta}$$
$$K3 = \frac{\beta M(i,j)S_i}{N_j}\left(\frac{1}{\theta} + \frac{\kappa_m}{\gamma}\right)$$
$$K4 = \frac{\beta\kappa_m M(i,j)S_i}{N_j\gamma}$$
$$K5 = \frac{\beta M(i,j)S_i}{N_j}\left(\frac{1}{\theta} + \frac{\kappa_s}{\gamma}\right)$$
$$K6 = \frac{\beta\kappa_s M(i,j)S_i}{N_j\gamma}$$

The general form of the characteristic polynomial [34] of (3.18) is given by:

$$f(\lambda) = \lambda^n - (-1)^{n-1}\text{tr}(G)\lambda^{n-1} + ... + (-1)^n \det(G) \tag{3.19}$$

Here, tr(G) and $\det(G)$ are:

$$\text{tr}(G) = \sum_{j=1}^{5}\frac{\beta M(j,j)S_j}{N_j}\left(\frac{\alpha p(j)}{\eta} + \frac{1-p(j)}{\theta} + \frac{(p(j)-1)(\kappa_s(q(j)-1)-\kappa_m q(j))}{\gamma}\right),$$
$$\det(G) = 0$$

The dominant eigenvalue of equation 3.19 is defined as $\mathcal{R}_0$ (equation 3.17). Due to the complexity of this polynomial, it is difficult to explicitly state the $\mathcal{R}_0$ expression.

3.3.3 Herd immunity

Herd immunity is reached when a sufficient proportion of the susceptible population is immune (either through natural infection or vaccination) [35]. As the proportion of susceptible population fall below a certain threshold (the level of herd immunity), disease transmission declines and disease

approaches extinction [35]. In simple homogeneous models, the herd immunity threshold is only dependent on the $\mathcal{R}_0$ value and can be mathematically expressed as [35]:

$$\text{Herd Immunity Threshold} = 1 - \frac{1}{\mathcal{R}_0} \tag{3.20}$$

However, in models with heterogeneity of population demographics (e.g., age) and contact patterns, the herd immunity threshold may differ [36, 37]. Using equation (3.20), the herd immunity threshold is 60% for $\mathcal{R}_0 = 2.5$. However, in heterogeneous settings, the herd immunity may be lower than 50%, but may also vary when considering real-world behavioral aspects (e.g., "super spreader events") [38, 39].

Chapter 4

Model parameterization and implementation

In this chapter, details of parameter values and distributions are provided in 4.1. The contact rates of different age-groups within the community and household are described in section 4.2. A non-standard finite difference method is used to simulate the model (3.1) - (3.13) and is shown in section 4.3. The model calibration and implementation are detailed in sections 4.4 and 4.5.

4.1 Model parameterization

To parameterize the model, we rely on recent estimates of COVID-19 characteristics, which were used in similar modelling studies [30]. The incubation period was sampled from a log-normal distribution with mean and standard deviation of 5.2 days and 0.1 days, respectively[10]; this period was truncated between 4 to 7 days. The pre-symptomatic period ($1/\theta$ days) was sampled from a gamma distribution with mean of 1.73 days (shape $= 1.058$ days and scale $= 2.174$ days) [22]; this period was also truncated between 0.8 to 3 days. The latent period ($1/\sigma$ days) was calculated by subtracting the pre-symptomatic period from the incubation period, which ranges from 1 to 6.2 days. The infectious period for asymptomatic individuals was sampled from a gamma distribution with mean of 5 days (shape $= 5$ days and scale $= 1$ day) [40, 41]. We parameterized the infectivity

in symptomatic and asymptomatic stages of infection relative to the pre-symptomatic stage. The relative infectivity were 11% [21], 44% [21, 22], and 89% [21, 28, 42] for asymptomatic, mild symptomatic, severe symptomatic stages as compared to pre-symptomatic stage. The infectious period following the onset of symptoms was sampled from a gamma distribution with mean of 3.67 days (shape $= 2.768$ and scale $= 1.1563$ days) [41]. The duration of hospitalization for non-ICU and ICU cases was sampled from a gamma distribution with mean of 11.75 days and 13.76 days respectively [43, 44]. The time period from hospitalization to death was sampled from a gamma distribution with a mean of 10.82 days[43, 44]. We assumed that individuals who recovered after the infectious period were no longer susceptible to the disease. Tables 4.1 and 4.2 summarize the parameter values.

4.2 Population mixing patterns

The population was subdivided into five age-groups: $0-4$, $5-19$, $20-49$, $50-64$, and ≥ 65 years. To account for the age-specific mixing patterns of individuals, two contact matrices were used: (i) the community contact matrix (M) ,and (ii) household contact matrix ($\tilde{M}$). These contact matrices were taken from a similar modelling study [30], and were derived from a study on contact patterns in urban populations [46] and during lockdown [47]. As summarized in table 4.3, the total number of daily contacts for each age-group was sampled from a negative binomial distribution for both non-isolated and isolated individuals. These were multiplied by the proportion of daily contacts for each age-group to distribute the number of contacts per-day between and within the different age-groups.

4.3 Non-standard method for numerical solutions

A simple first-order non-standard finite-difference method was used to obtain the numerical solutions of the deterministic compartmental model (3.1). This method preserves the positivity of solutions which is a requirement for this epidemic model [48]. To develop the method, the time interval was

Table 4.1: The parameter values and distributions of this model. The transmission probability was calibrated to obtain a 60% herd immunity for the baseline scenario.

Description	Variable	Age-Groups					Reference
		$0-4$	$5-19$	$20-49$	$50-65$	≥ 65	
Transmission probability per contact during pre-symptomatic period	β	0.0473					Calibrated to $R_0 = 2.5$ [10, 45]
Relative transmissibility of mild symptomatic cases compared to pre-symptomatic cases	κ_m	0.44					[21, 22]
Relative transmissibility of severe symptomatic cases compared to pre-symptomatic cases	κ_s	0.89					[21, 28, 42]
Relative transmissibility of asymptomatic cases compared to pre-symptomatic cases	α	0.11					[21]
Proportion of asymptomatic cases	p_a	0.3	0.31	0.29	0.29	0.18	[26, 27]
Proportion of mild symptomatic cases	q_a	0.95	0.9	0.85	0.6	0.2	[28, 42]
Proportion of mild symptomatic cases that self-isolate	f_a	0.2					Assumed
Proportion of severe symptomatic cases that self-isolate	g_a	1.0					Assumed
Proportion of non-ICU cases	h_a	0.09	0.09	0.09	0.19	0.235	
Proportion of ICU cases	c_a	0.01	0.02	0.05	0.197	0.26	
Proportion of non-ICU cases that result in death	d_a	0.0002	0.0007	0.0035	0.04275	0.2895	
Proportion of ICU cases that result in death	m_a	0.0002	0.0007	0.0035	0.04275	0.2895	

Table 4.2: The average duration of epidemiological periods and hospital stays.

Description	Variable	Value or Distribution	Range	Reference
Incubation period	$\frac{1}{\sigma}+\frac{1}{\theta}$	LogNormal$(5.2, 0.1)$	Truncated $4-7$ days	[10, 24]
Pre-symptomatic period	$\frac{1}{\theta}$	Gamma(shape: 1.058, scale: 2.174)	Truncated $1-3$ days	Derived from [22]
Symptomatic period	$\frac{1}{\gamma}$	Gamma(shape: 2.768, scale: 1.1563)	Truncated ≥ 1.5 days	Estimated from [41]
Asymptomatic period	$\frac{1}{\eta}$	Gamma(shape: 5, scale: 1)	Not truncated	Derived from [21]
Latent period	$\frac{1}{\sigma}$	Incubation period − Pre-symptomatic Period	$1-6$ days	Calculated
Time from symptom onset to self-isolation	$\frac{1}{\tau}$	1 day	Constant	Assumed
Time from symptom onset to hospitalization	$\frac{1}{\delta}$	Unif$(2, 5)$	Not truncated	[43]
Time from hospitalization to death	$\frac{1}{\mu}$	Gamma(shape: 4.5,scale: 2.75)	Truncated $7-15$ days	[43, 44]
Length of non-ICU stay	$\frac{1}{\phi}$	Gamma(shape: 5.3,scale: 2.1)	Truncated $8-17$ days	[43, 44]
Length of ICU stay	$\frac{1}{\psi}$	Gamma(shape: 4.5,scale: 2.75)	Truncated $10-19$ days	[43, 44]

Table 4.3: The daily proportion of contacts between and within different age-groups. The daily number of contacts for each age-group were sampled from a negative binomial distribution with mean and standard deviation shown below for non-isolated and isolated individuals.

Age group	**Proportion of contacts between and within age-groups**					**Total daily contacts for non-isolated individuals**		**Total daily contacts for isolated individuals**	
	$\mathbf{0-4}$	$\mathbf{5-19}$	$\mathbf{20-49}$	$\mathbf{50-65}$	$\mathbf{\geq 65}$	**Mean**	**(SD)**	**Mean**	**(SD)**
$\mathbf{0-4}$	0.2287	0.1839	0.4219	0.1116	0.0539	10.21	(7.65)	2.86	(2.14)
$\mathbf{5-19}$	0.0276	0.5964	0.2878	0.0591	0.0291	16.793	(11.7201)	4.70	(3.28)
$\mathbf{20-49}$	0.0276	0.5964	0.2878	0.0591	0.0291	16.793	(11.7201)	4.70	(3.28)
$\mathbf{50-64}$	0.0242	0.1094	0.4867	0.2723	0.1074	11.2669	(9.5935)	3.15	(2.66)
$\mathbf{\geq 65}$	0.0207	0.1083	0.4071	0.2193	0.2446	8.0027	(6.9638)	2.24	(1.95)

discretized between 0 to 500 days with a fixed step-size of 1 day. For each variable X_i (i.e., one of the epidemiological states of the system) that is approximated, there were three rules that were applied [48]. First, a negative term of X_i was written at the advanced time-step [48]. Second, if order of X_i is n, where n is an integer greater than 1, then X_i^n was split into two components, such as $X_i^1 * X_i^{(n-1)}$ [48]. Here, X_i^1 was written at the advanced time-step and $X_i^{(n-1)}$ was written at the current time-step [48]. Third, all other variables X_j, where $j \neq i$ are written at current time step [48]. The numerical solutions of (3.1) can then be described by:

$$
\begin{aligned}
x(t) &= \beta \sum_{j=1}^{5} M_{a,j} \frac{(P_{m,j}(t) + P_{s,j}(t) + \kappa_m I_{m,j}(t) + \kappa_s I_{s,j}(t) + \alpha A_j(t))}{N_j} \\
y(t) &= \beta \sum_{j=1}^{5} \tilde{M}_{a,j} \frac{(\kappa_m Q_{m,j}(t) + \kappa_s Q_{s,j}(t))}{N_j} \\
S_a(t+h) &= \frac{S_a(t)}{1 + hx(t) + hy(t)} \\
E_a(t+h) &= \frac{E_a(t) + hS_a(t)(x(t) + y(t))}{1 + h\sigma} \\
A_a(t+h) &= \frac{A_a(t) + hp_a\sigma E_a}{1 + h\eta} \\
P_{m,a}(t+h) &= \frac{P_{m,a}(t) + h(1-p_a)q_a\sigma E_a}{(1 + h\theta)} \\
I_{m,a}(t+h) &= \frac{I_{m,a}(t) + h\theta P_{m,a}(t)}{1 + h(1-f_a)\gamma + hf_a\tau} \\
Q_{m,a}(t+h) &= \frac{Q_{m,a}(t) + hf_a\tau I_{m,a}(t)}{1 + h\gamma(\frac{\tau}{\tau-\gamma})} \\
P_{s,a}(t+h) &= \frac{P_{s,a}(t) + h(1-p_a)(1-q_a)\sigma E_a}{(1 + h\theta)} \\
I_{s,a}(t+h) &= \frac{I_{s,a}(t) + h\theta P_{s,a}(t)}{(1 + h(1-g_a-h_a)\gamma + hg_a\tau + hh_a\delta)} \\
Q_{s,a}(t+h) &= \frac{Q_{s,a}(t) + hg_a\tau I_{s,a}(t)}{1 + h\gamma(\frac{\tau}{\tau-\gamma})} \\
H_a(t+h) &= \frac{H_a(t) + h(1-c_a)h_a\delta I_{s,a}(t)}{1 + hd_a\mu + h(1-d_a)\phi} \\
C_a(t+h) &= \frac{C_a(t) + hc_a h_a\delta I_{s,a}(t)}{1 + hc_a\mu + h(1-c_a)\psi}
\end{aligned}
$$

$$
\begin{aligned}
R_a(t+h) &= R_a(t) + h(\eta A_a(t) + \gamma \left(\frac{\tau}{\tau-\mu}\right)(Q_{s,a}(t) + Q_{m,a}(t)) \\
&\quad +(1-d_a)\phi H_a(t) + (1-m_a)\psi C_a(t) + (1-f_a)\gamma I_{m,a}(t) \\
&\quad +(1-g_a-h_a)\gamma I_{s,a}(t)) \\
D_a(t+h) &= D_a(t) + h(d_a\mu H_a(t) + m_a\mu C_a(t))
\end{aligned}
$$

where h is the time-step.

4.4 Estimating β and $\mathcal{R}_0$

The β value was varied until the herd immunity of 60% was achieved for the baseline scenario (no intervention measure) and parameters f_a, g_a, c_a, and h_a were set to zero. To find the herd immunity, the average number of recovered individuals over a 500 day period for 1000 simulations was divided by the total population (10,000 individuals). Using this approach, $\beta = 0.0473$.

The average $\mathcal{R}_0$ value was calculated using $\beta = 0.0473$, parameter values from tables 4.1 and 4.3, and the next generation method shown in section 3.3. The average $\mathcal{R}_0$ value was approximately 2.48 (IQR: 2.46 to 2.50) and is shown in figure 4.1. This calculation of $\mathcal{R}_0$ averaged the results of 2000 simulations and used bootstrap sampling to obtain the median and interquartile range (IQR), with 1000 replicates for average of reproduction number.

4.5 Model implementation

Monte-Carlo simulations were used to derive a range of possible outcomes and account for the uncertainty in the parameter values. For each simulation, one exposed individual was introduced into each age-group and the model was simulated for 500 days. The results of 1000 simulations were averaged for the outcomes of interest (infections, hospitalizations, and deaths). Bootstrap sampling was used to obtain the median and interquartile range (IQR), with 500 replicates for the mean of cumulative infections, hospitalizations, and deaths. The numerical methods was implemented in MATLAB©.

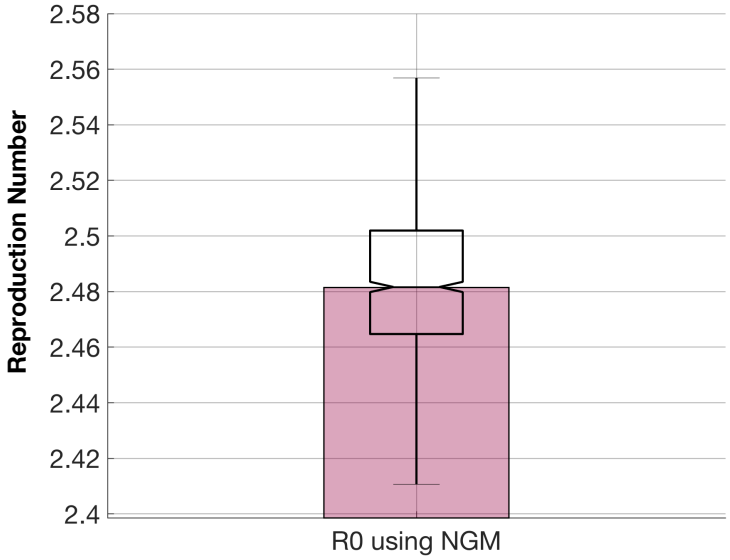

Figure 4.1: The average reproduction number (R0) calculated using the next generation method (NGM).

Chapter 5

Scenarios and efficiency analyses

5.1 Scenarios

We simulated the model to evaluate the outcomes of six scenarios including, self-isolation of infected individuals and age-specific stay-at-home orders. Scenario 1 (S1) includes self-isolation of infected individuals, while scenarios 2 to 6 combine S1 with stay-at-home orders for particular age-groups. Scenario 3 to 6 were designed to target age groups other than $20-49$ years old. It is important to note that scenarios S2 to S6 have self-isolation of 20% mild cases and 100% severe cases from the start to end of simulations, and the stay-at-home order starts on day 30. Summary of scenarios are provided in Table 5.1, with the following details considered in simulations:

1. **Base Scenario (S0)**: This includes no intervention measure, implying that interactions between susceptible and infectious individuals was governed by the community contact matrix, without self-isolation of infected individuals.

2. **Scenario (S1)**: The only intervention measure was self-isolation of 20% mildly symptomatic cases and 100% of severe cases for the entire duration of the infectious period. This included all age-groups and the percentage of the population practising self-isolation would vary for each simulation depending on the number of cases with mild and severe illness.

3. **Scenario (S2)**: There were two intervention measures considered: (i) self-isolation of mild (20%) and severe (100%) cases, and (ii) stay-at-home orders for all age-groups for a duration of: a) 90 days, and b) 150 days, corresponding to lockdown scenarios.

4. **Scenario (S3)**: Similar intervention measures as S2 were considered, while stay-at-home order was targeted only to individuals ≥ 65 years of age. The stay-at-home order was practised by 17% of the total population.

5. **Scenario (S4)**: Similar intervention measures as S2 were considered, while stay-at-home order was targeted to individuals 50 years and older. The stay-at-home order in this scenario was practised by 37% of the total population.

6. **Scenario (S5)**: Similar intervention measures as S2, with the difference that the stay-at-home order was targeted to individuals $5-19$ years for a duration of: (a) 30 days, (b) 60 days, (c) 120 days, and (d) 240 days. This is the school closure scenario which targets children (17% of the total population).

7. **Scenario (S6)**: A combination of intervention measures from scenario 4 and scenario 5 were considered. In general, the two main intervention measures were: (i) self-isolation of mild (20%) and severe (100%) cases, and (ii) stay-at-home orders for individuals aged $5-19$ years and individuals ≥ 50 years. Since stay-at-home order targeted three age-groups, this scenario accounted for 54% of the total population.

   (a) individuals ≥ 50 years stay-at-home for 90 days and school closure for 30 days

   (b) individuals ≥ 50 years stay-at-home for 90 days and school closure for 60 days

   (c) individuals ≥ 50 years stay-at-home for 90 days and school closure for 120 days

   (d) individuals ≥ 50 years stay-at-home for 90 days and school closure for 240 days

   (e) individuals ≥ 50 years stay-at-home for 150 days and school closure for 30 days

   (f) individuals ≥ 50 years stay-at-home for 150 days and school closure for 60 days

   (g) individuals ≥ 50 years stay-at-home for 150 days and school closure for 120 days

(h) individuals ≥ 50 years stay-at-home for 150 days and school closure for 240 days

5.2 Efficiency

The approach used to calculate efficiency of stay-at-home scenarios is proposed in [30] and utilizes the following efficiency formula:

$$E_s = \frac{\text{Cumulative number of outcomes averted}}{\text{The proportion of the population following stay-at-home order}}$$

This ratio determines the number of outcomes such as infections, hospitalizations, or deaths averted per individual practicing stay-at-home order. Since the disease dynamics are affected by the implementation of different interventions, the number of outcomes averted during the entire simulation timelines were used rather than just the time-period of the stay-at-home order.

Table 5.1: Description of simulated Scenarios.The last column shows the percentage of population practising the stay-at-home order (SAHO).

Scenario	Type of Intervention	Age Group	Proportion practicing	Duration of intervention	% practising SAHO
S0 (Baseline)	None	-	-	-	-
S1	Self-isolation	All	20% of mild cases 100% of severe cases	Infectious period	varies
S2 (Lockdown)	S1 + stay-at-home	All	100%	a) 90 days	100%
				b) 150 days	
S3	S1 + stay-at-home	65+ years old	100%	Same as S2	17%
S4	S1 + stay-at-home	50+ years old	100%	Same as S2	37%
S5	S1 + school closure	5 − 19 years old	100%	a) 30 days	17%
				b) 60 days	
				c) 120 days	
				d) 240 days	
S6	S4 + S5	50+ years old	100%	Same as S4, S5	54%
		5-19 years old			

Chapter 6

Results

This chapter details the results of scenarios defined in the previous chapter. These results are presented as the average of 1000 simulations for each scenario in a synthetic population of 10,000 individuals. The stratification of model population is based on the demographics of Ontario, Canada. Simulations were run for 500 days, with a time-step of one-day. Outcomes were derived for the incidence of infection (i.e., daily number of new infections), hospitalizations, and deaths.

6.1 Baseline scenario, S0

In the absence of any intervention measure, the peak of incidence occurs on day 80 with 72 infections. Age-group $20-49$ years had the highest cumulative infections, with 2526.8 (Interquartile range, IQR: 2507.1 to 2549.3) infections. Individuals in age-groups ≥ 50 years had the most hospitalizations and deaths. The total incidence of hospitalizations peaked on day 92, with 2.5 non-ICU cases and 0.7 ICU cases per 10,000 populations. The highest cumulative hospitalizations were seen in age-group ≥ 65 years, with 106.7 (IQR: 105.0 to 108.3) non-ICU cases and 37.5 (IQR: 36.8 to 38.1) ICU cases. This age-group (≥ 65 years) also had the most number of deaths, with 46.4 (IQR: 45.6 to 47.0) cumulative deaths per 10,000 population. The peak incidence of deaths occurred on day 105 with 0.6 deaths per 10,000 population. The results of this scenario are shown in figure 6.1.

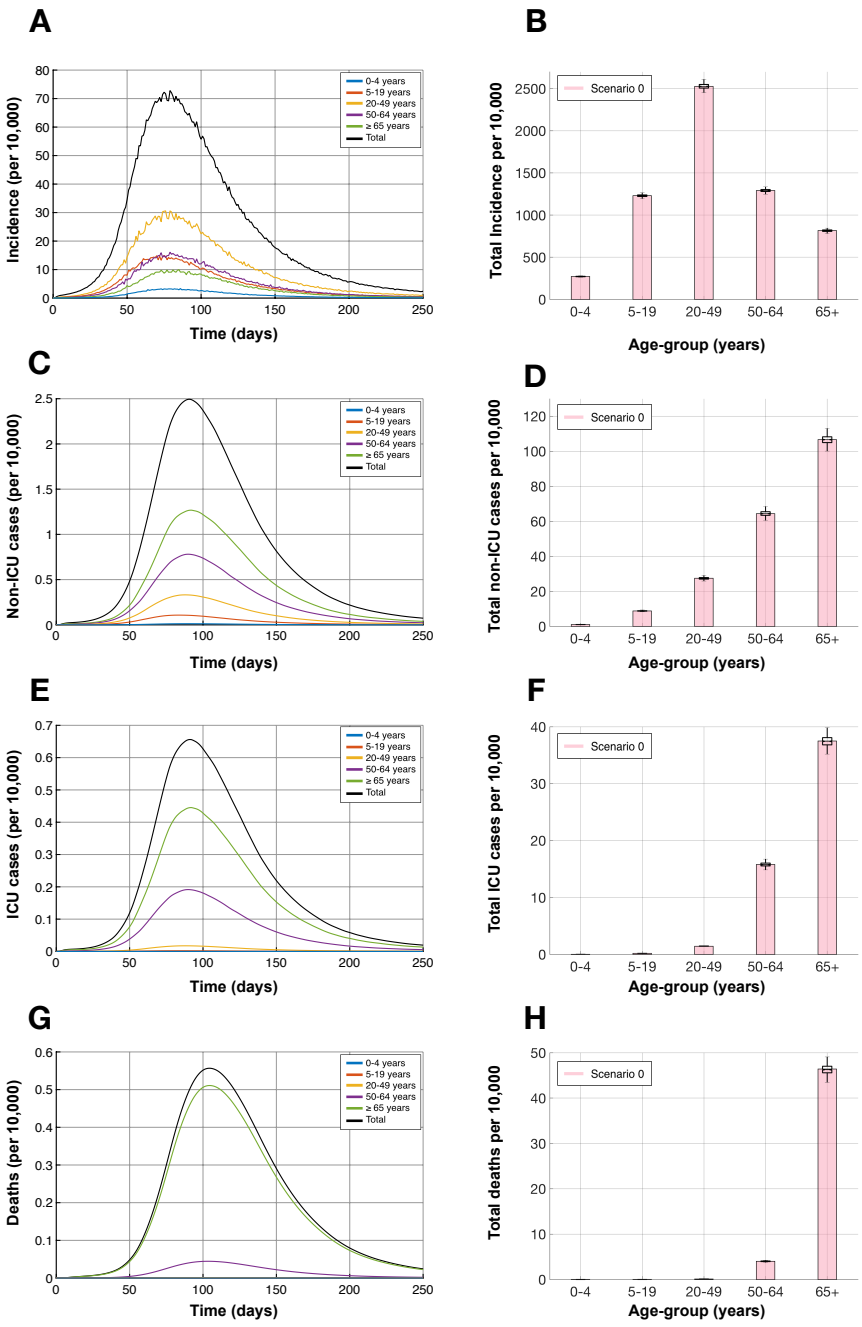

Figure 6.1: The average projected curves for daily incidence of infections (A), non-ICU cases (C), ICU cases (E), and deaths (G) for the baseline scenario, S0. In addition, the cumulative incidence (B), cumulative non-ICU cases (D), cumulative ICU cases (F), and cumulative deaths (H) over a 500 day period are shown for the baseline scenario. For graphs B,D,F, and H, the bars show the mean values and the boxplots show the median and IQR values. These estimates and projections are per 10,000 population.

6.2 Scenario S1

As 20% of mild cases and 100% of severe non-hospitalized cases were self-isolated after one day of symptom onset, the peak incidence reduced to 45.6 infections ($\approx 37\%$ reduction at the peak compared to S0) per 10,000 population. The highest cumulative incidence was found in age-group $20-49$ years old, with 1887.3 (IQR: 1863.3 to 1910.8) infections per 10,000 population. The number of hospitalized cases peaked on day 99 (delayed by one week as compared to S0), with 0.4 non-ICU cases and 0.1 ICU cases per 10,000 population. This corresponded to $\approx 84\%$ reduction at the peak of hospitalizations as compared to S0. Age-group ≥ 65 years had the most hospitalizations, with 19.8 (IQR: 19.5 to 20.1) non-ICU cases and 6.9 (IQR: 6.8 to 7.0) ICU cases per 10,000 population. The peak incidence of deaths was delayed by one week to day 112, and reduced to 0.1 (corresponding to $\approx 84\%$ reduction compared to S0) deaths at the peak per 10,000 population. Age-group ≥ 65 years still had the highest cumulative deaths, with 8.6 (IQR: 8.5 to 8.8) deaths per 10,000 population. The results of this scenario are shown in figure 6.2.

6.3 Scenario S2

Lockdown orders were effective in reducing the total peak incidence of infections, hospitalizations, and deaths. Disease incidence declined significantly during the entire lockdown period and was followed by a surge in infections, hospitalizations, and deaths after the lockdown was relaxed. For scenario S2a, the peak incidence occurred on day 240 (120 days after lockdown ended) with 24.1 infections, while for S2b, the peak incidence occurred on day 345 (165 days after lockdown ended) with 16.6 infections per 10,000 population. This corresponded to $\approx 67\%$ and $\approx 77\%$ reduction in peak incidence for S2a and S2b, respectively, as compared to the baseline scenario S0; and $\approx 47\%$ and $\approx 64\%$ reduction in peak incidence for S2a and S2b, respectively, as compared to $S1$. Notably, the incidence curves for age-groups $5-19$ years old and $50-64$ years old were almost identical after the lockdown period ended for both scenarios S2a and S2b. For S2a, hospitalizations peaked at 0.2 non-ICU cases and 0.05 ICU cases, whereas for S2b, the peak in hospitalized cases further declined to 0.1 non-ICU cases and 0.04 ICU cases, respectively, per 10,000 population. The number

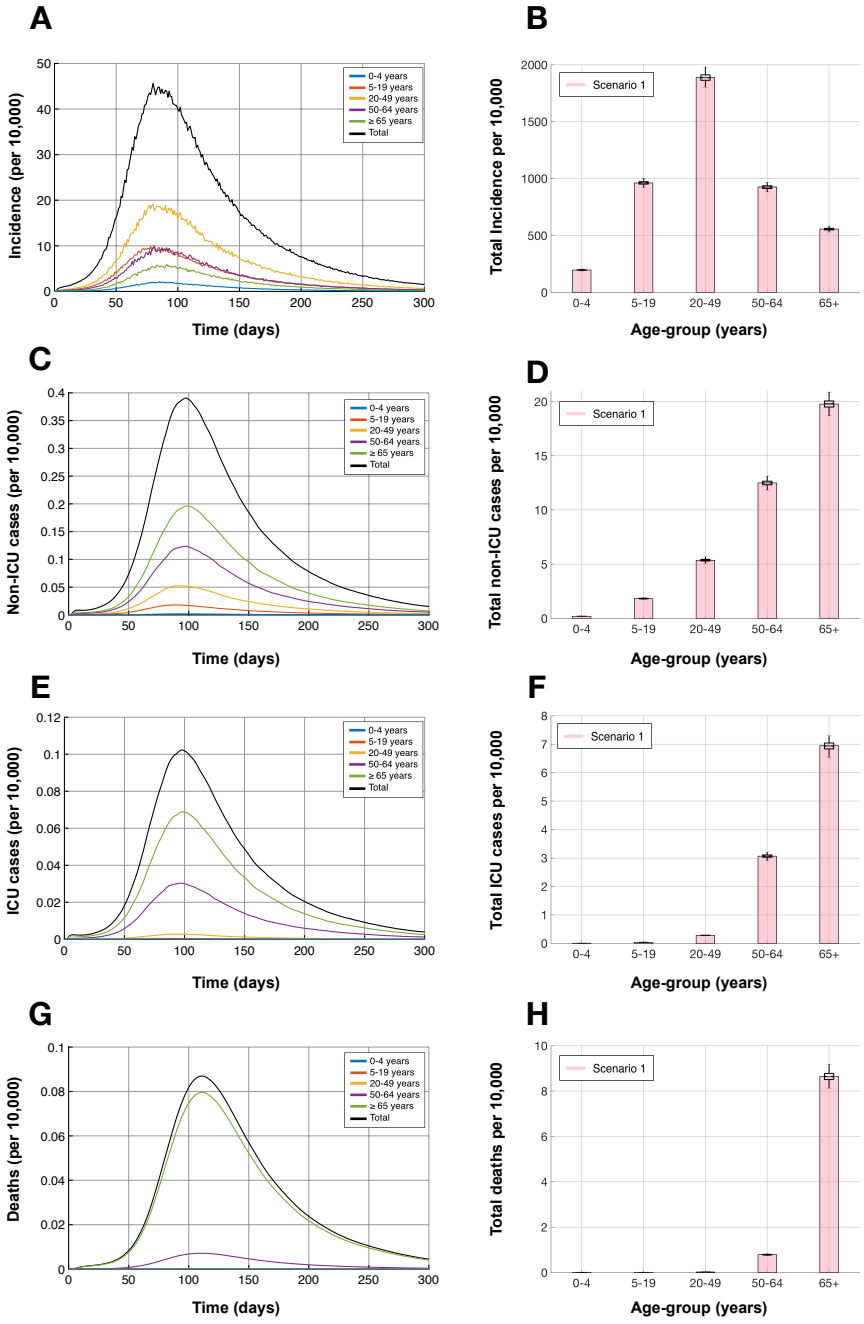

Figure 6.2: The average projected curves for daily incidence of infections (A), non-ICU cases (C), ICU cases (E), and deaths (G) for S1. In addition, the cumulative incidence (B), cumulative non-ICU cases (D), cumulative ICU cases (F), and cumulative deaths (H) over a 500 day period are shown for S1. For graphs B,D,F, and H, the bars show the mean values and the boxplots show the median and IQR values. These estimates and projections are per 10,000 population.

of deaths peaked at 0.05 ($\approx 92\%$ reduction compared to S0) for S2a and 0.03 ($\approx 94\%$ reduction compared to S0) for S2b per 10,000 population. For both scenarios, the epidemic continued past 500 days, which implied that the cumulative infections, hospitalizations, and deaths would increase and may be higher than shown in figure 6.3. The results of this scenario are shown in figure 6.3.

6.4 Scenario S3

This scenario targeted individuals 65 years and older for a stay-at-home order for 3 months and 5 months. Although extending the stay-at-home order from 3 months (S3a) to 5 months (S3b) did not have a significant effect on reducing the peak incidence, it reduced the cumulative hospitalizations and deaths, especially amongst the targeted age group. Specifically, a 3-month and a 5-month stay-at-home order reduced the peak incidence to 42.4 ($\approx 7\%$ reduction as compared to S1) and 42.0 ($\approx 8\%$ reduction as compared to S1) infections, respectively per 10,000 population. For a 3-month (S3a) stay-at-home order, the cumulative incidence, hospitalizations, and deaths for individuals aged 65 and older were 378.3 (IQR: 374.2 to 382.5) infections, 13.3 (IQR: 13.1 to 13.4) non-ICU cases, 4.7 (IQR: 4.6 to 4.7) ICU cases, and 5.8 (IQR: 5.7 to 5.8) deaths, per 10,000 population. Extending the stay-at-home order to 5 months (S3b) for individuals aged 65 and older reduced the cumulative outcomes of interest to 272.5 (IQR: 269.3 to 275.1) infections, 9.5 (IQR: 9.39 to 9.7) non-ICU cases, 3.3 (IQR: 3.3 to 3.4) ICU cases, and 4.12 (IQR: 4.06 to 4.16) deaths.

Notably, hospitalizations for S3a displayed two peaks; the first peak (≈ 0.26 non-ICU cases and ≈ 0.06 ICU cases at the peak per 10,000 population) occurred during the stay-at-home period which was followed by a second peak (≈ 0.23 non-ICU cases and ≈ 0.06 ICU cases per 10,000 population) after the stay-at-home period ended, as shown in figure 6.4. In contrast, a 5-month stay-at-home order only resulted in a slight increase in the number of hospitalizations after the stay-at-home period ended, where the magnitude of this second peak was significantly less compared to the first peak in hospitalizations. These results suggest that a 3-month duration may be sub-optimal due to the emergence of a second peak in hospitalizations and deaths. A similar trend is observed for the daily number of deaths for S3a and S3b. For S3a, the number of

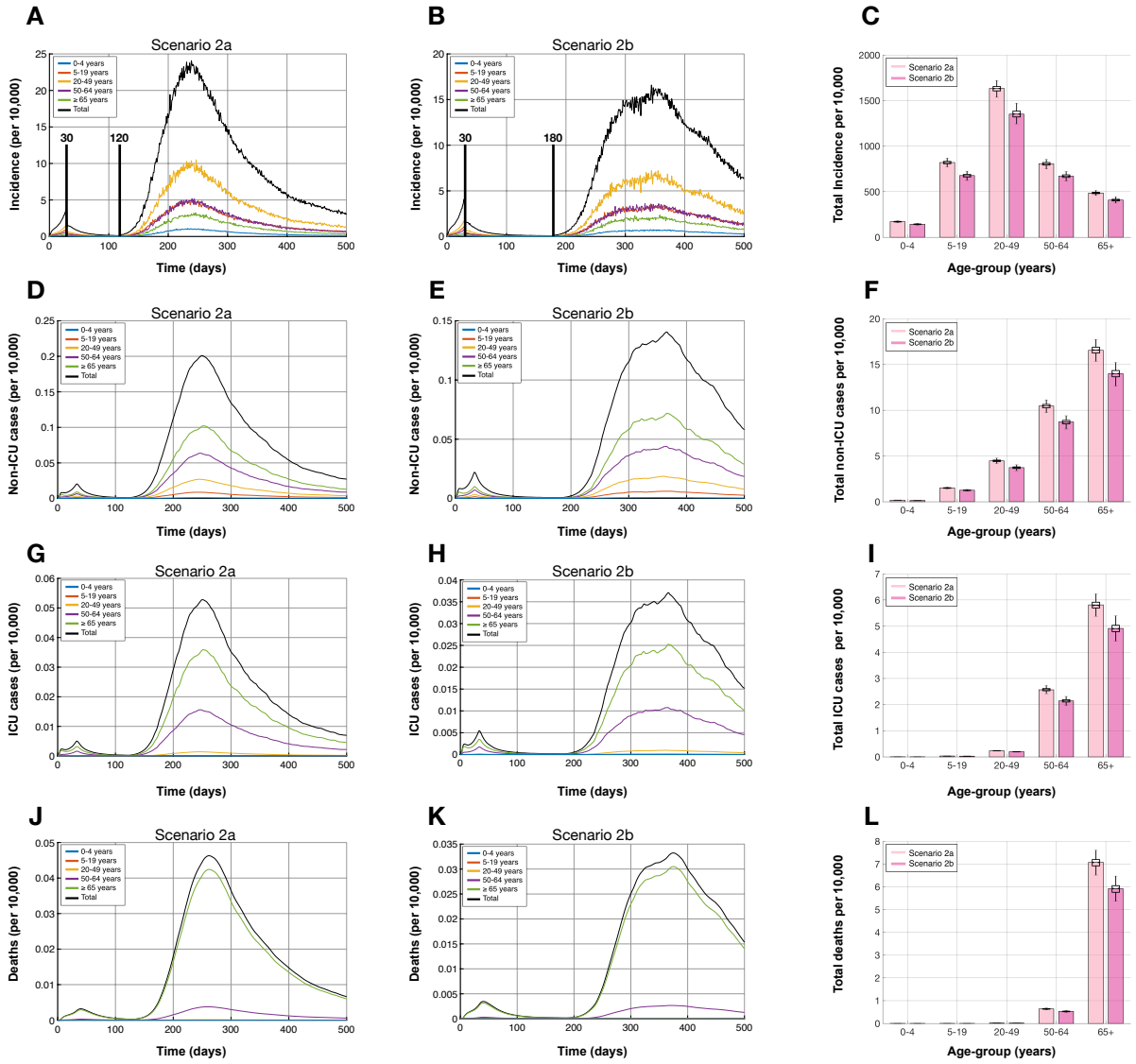

Figure 6.3: The average projected curves for daily incidence (A and B), non-ICU cases (D and E), ICU cases (G and H), and deaths (J and K) for S2a and S2b. The vertical bars in A and B show the start and end of the stay-at-home order for each scenario. The cumulative incidence (C), cumulative non-ICU cases (F), cumulative ICU cases (I), and cumulative deaths (L) are shown for S2a and S2b. For graphs C,F,I, and L, the bars show the mean values and the boxplots show the median and IQR values. These estimates and projections are per 10,000 population.

deaths peaked during the second wave on day 151 with 0.05 deaths per 10,000 population after the stay-at-home order ended. For S3b, the number of deaths peaked on day 116 with 0.04 deaths

per 10,000 population during the stay-at-home period, which corresponds to approximately 31% reduction as compared S3a. For S3b, there was an increase in the number of deaths after the stay-at-home period ended, but second peak was significantly lower in magnitude with less than 0.02 deaths per 10,000 population. We found that S3b outperformed S3a in reducing the cumulative hospitalizations and deaths, as well as peak incidence of hospitalized cases and deaths. The results of these scenarios are shown in figure 6.4.

6.5 Scenario S4

By targeting the age-group 50-64 years old in addition to those 65 years and older for a stay-at-home order, the peak incidence fell below 30 infections for both S4a and S4b. Specifically, extending the stay-at-home order from 3 months (S4a) to 5 months (S4b) reduced the peak incidence from 29 ($\approx 36\%$ reduction) infections to 27.9 ($\approx 39\%$ reduction) infections per 10,000 population, as compared to S1. Notably, both scenarios resulted in an immediate rise in disease incidence after the stay-at-home period ended, where the magnitude of the second peak in S4a (≈ 24 infections) was greater than the magnitude of the second peak in S4b (≈ 8 infections). The hospitalization dynamics of these scenarios were very similar to S3a and S3b. For this scenario, the highest number of hospitalized cases for S4a occurred during the second peak (after the stay-at-home period ended) with 0.2 ($\approx 46\%$ reduction compared to S1) non-ICU cases and 0.06 ($\approx 43\%$ reduction compared to S1) ICU cases per 10,000 population. In contrast, for S4b, the highest number of hospitalized cases occurred during the first peak (within the stay-at-home period) with 0.13 ($\approx 67\%$ reduction compared to S1) non-ICU cases and 0.03 ($\approx 73\%$ reduction compared to S1) ICU cases per 10,000 population. For S4a, the number of deaths peaked on day 162 with 0.05 deaths per 10,000 population, while S4b had two peaks in the number of deaths, both were less than 0.02 deaths per 10,000 population. Overall, S4b outperformed S4a as it reduced hospitalizations and deaths (both cumulative and peak incidence), especially for age-group ≥ 50 years. A key observation was that the duration of a stay-at-home order affected the magnitude of the peak incidence of infections, hospitalizations, and deaths, as shown in figures 6.4 and 6.5.

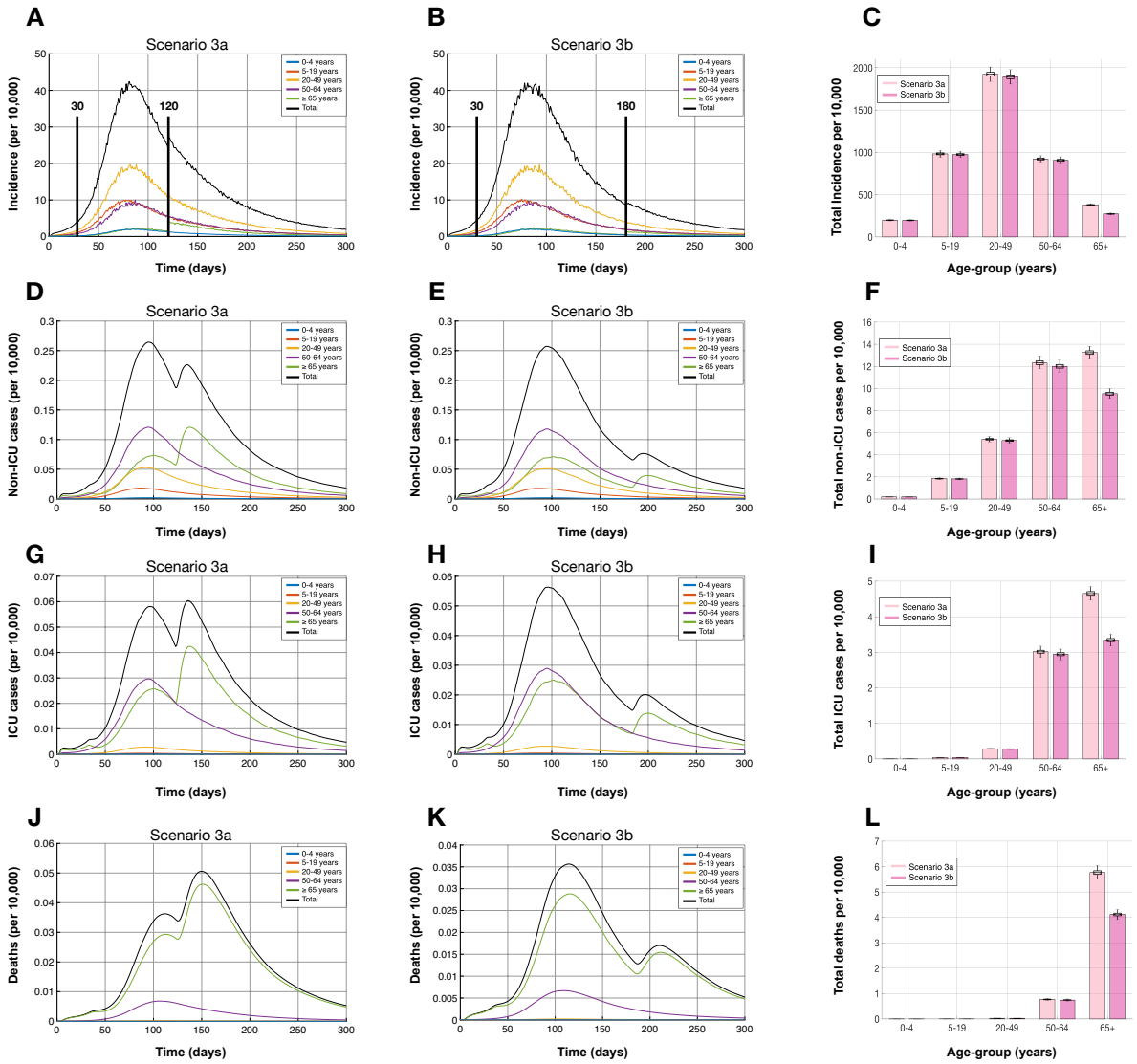

Figure 6.4: The average projected curves for daily incidence (A and B), non-ICU cases (D and E), ICU cases (G and H), and deaths (J and K) for S3a and S3b. The vertical bars in A and B show the start and end of the stay-at-home order for each scenario. The cumulative incidence (C), cumulative non-ICU cases (F), cumulative ICU cases (I), and cumulative deaths (L) are shown for S3a and S3b. For graphs C,F,I, and L, the bars show the mean values and the boxplots show the median and IQR values. These estimates and projections are per 10,000 population.

6.6 Scenario S5

School closure represents a stay-at-home order for individuals aged 5-19 years, was effective at reducing peak incidence when it was implemented for a duration longer than 4 months in S5c and

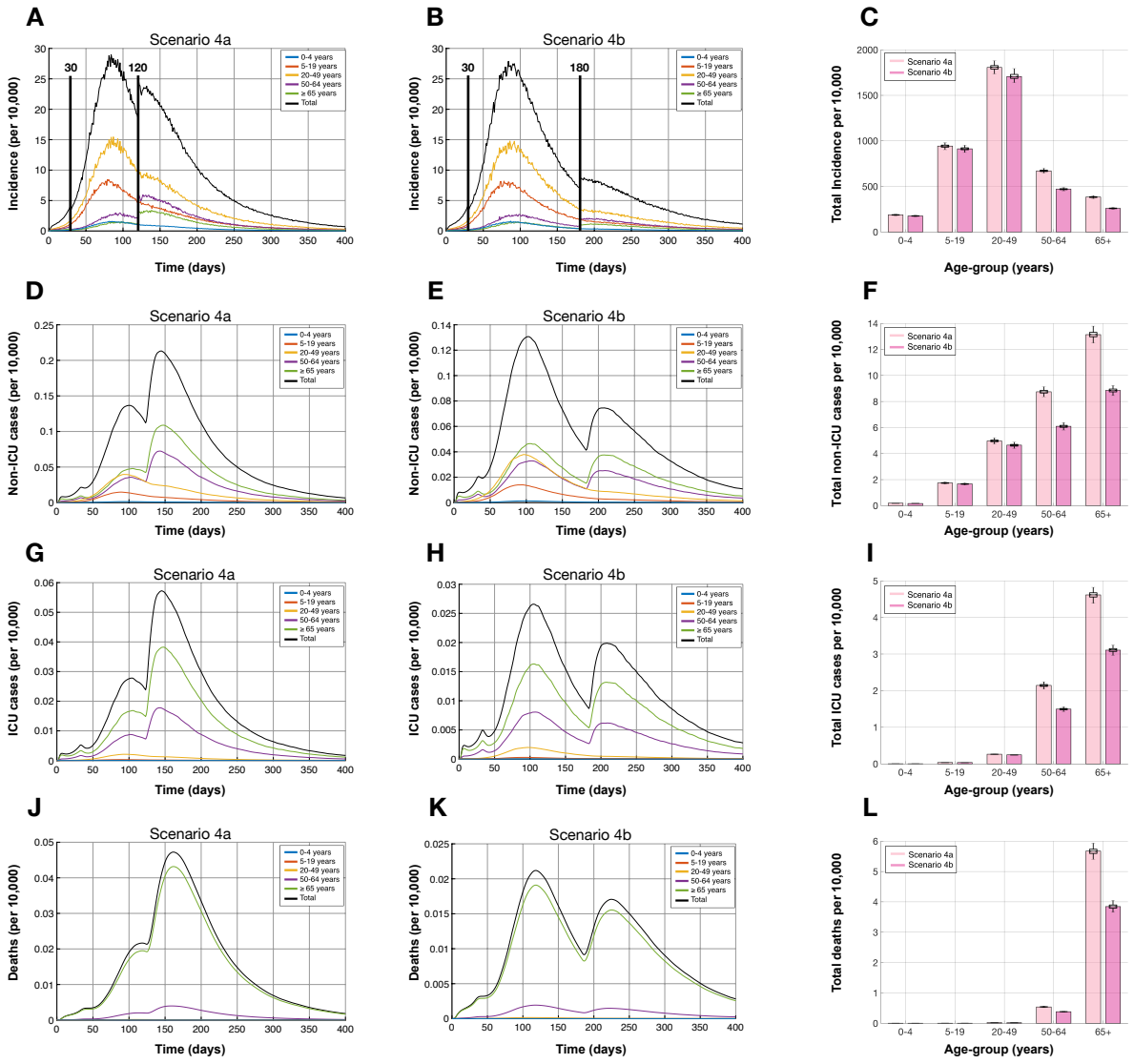

Figure 6.5: The average projected curves for daily incidence (A and B), non-ICU cases (D and E), ICU cases (G and H), and deaths (J and K) for S4a and S4b. The vertical bars in A and B show the start and end of the stay-at-home order for each scenario. The cumulative incidence (C), cumulative non-ICU cases (F), cumulative ICU cases (I), and cumulative deaths (L) are shown for S4a and S4b. For graphs C,F,I, and L, the bars show the mean values and the boxplots show the median and IQR values. These estimates and projections are per 10,000 population.

8 months in S5d. The longest delay in outbreak peak was observed for a 2-month school closure, where peak incidence occurred on day 117 with 35.8 ($\approx 21\%$ reduction compared to S1) infections

per 10,000 population. Extending the school closure from 1 month to 8 months reduced peak incidence from 43 ($\approx 6\%$ reduction compared to S1) infections to 23.6 ($\approx 48\%$ reduction compared to S1) infections. The cumulative infections for each scenario in age-group $5-19$ years was: (i) 959.8 (IQR: 948.5 to 969.8) infections in S5a, (ii) 929.8 (IQR: 920.6 to 941.4) infections in S5b, (iii) 737.1 (IQR: 729.7 to 745.8) infections in S5c, and (iv) 473.4 (IQR: 467.2 to 479.4) infections in S5d. These results highlight that a 1-month or 2-month school closure under-performed in reducing the outcomes of interest. An important aspect to consider for a 4-month or 8-month school closure is the emergence of a second peak after the school closure period ended, where the magnitude of the second peak was reduced by approximately 10 and 16 infections per 10,000 population, respectively, as compared to the first peak. Although extending school closures to 4 months and 8 months reduced infections, it under-performed in reducing hospitalizations and deaths, especially compared to scenarios S3 and S4. This is in part explained by the fact that individuals in age-group $5-19$ years have fewer hospitalizations and mostly interact with individuals from their own age-group. Among all scenarios simulated here, an 8-month school closure exhibited the lowest number of hospitalized cases at the outbreak peak, with 0.2 ($\approx 44\%$ reduction as compared to S1) non-ICU cases and 0.06 ($\approx 41\%$ reduction compared to S1) ICU cases per 10,000 population on day 107. This scenario further reduced the cumulative hospitalizations in those 65 years and older, which is the age-group associated with the highest hospitalization and death rates, to 15.0 (IQR: 14.6 to 16.10) non-ICU cases and 5.6 (IQR: 5.5 to 5.6) ICU cases per 10,000 population. The lowest peak incidence of deaths was observed for S5d, with 0.05 ($\approx 43\%$ reduction compared to S1) deaths per 10,000 population. Furthermore, an 8-month school closure reduced the cumulative deaths for age-group ≥ 65 years to 6.8 (IQR: 6.7 to 6.9) deaths per 10,000 population, which was the lowest cumulative deaths amongst all scenarios. The results for this scenario are shown in figure 6.6.

To evaluate the effectiveness of school closure as compared to only self-isolation of infected individuals (S1), the percent reduction in cumulative infections, hospitalizations, and deaths for S5 was analyzed (figure 6.7). These results indicate that a shorter duration of school closure (i.e., 1 month or 2 months) under-performs in reducing the outcomes of interest. As shown in figure 6.7, an 8 month school closure was most effective, with over 23.4% reduction (IQR: 22.0% to 23.7%) in

infections, 20.7% reduction (IQR: 19.0% to 22.2%) in hospitalizations, and 21.2% reduction (IQR: 19.4% to 22.9%) in deaths.

6.7 Scenario S6

Combining a stay-at-home order for individuals ≥ 50 years with school closure reduced the peak of incidence below 32 infections for all scenarios. Combining an 8-month school closure with a stay-at-home order for age-group ≥ 50 years for 3 months (S6d) and 5 months (S6h) resulted in the lowest outbreak peak, with 13.4 ($\approx 54\%$ reduction compared to S4a) infections and 11.6($\approx 59\%$ reduction compared to S4b) infections per 10,000 population, respectively. Notably, extending the stay-at-home order for age-group ≥ 50 years from 3 months (S6a) to 5 months (S6e) in addition to a 1-month school closure was the most effective at reducing the cumulative infections in older age-groups, leading to 533.2 (IQR: 527.3 to 539.1) infections for age-group $50-64$ years and 296.3 (IQR: 292.8 to 299.9) infections for age-group ≥ 65 years per 10,000 population. Furthermore, S6e had the lowest cumulative hospitalizations and deaths in age-group ≥ 65 years, with 10.2 (IQR: 10.1 to 10.3) non-ICU cases, 3.6 (IQR: 3.5 to 3.6) ICU cases, and 4.4 (IQR: 4.3 to 4.5) deaths, per 10,000 population. Extending school closures to 8 months (S6d and S6h) resulted in the emergence of second or third wave in infections and the cumulative infections, hospitalizations, and deaths shown for S6d and S6h were an underestimate as the epidemic continued past 500 days. The results of this scenario are shown in figure 6.8 and figure 6.9.

To evaluate the effectiveness of S6 as compared to S4, the percent reduction in cumulative infections, hospitalizations, and deaths was calculated and is shown in figure 6.10. These findings indicate that S6 under-performed as compared to S4. In figure 6.10, both scenarios S6d and S6h resulted in a percent decrease in infections as compared to S4, because the cumulative infections were underestimated due to the continued outbreak past 500 days. Although a stay-at-home order for individuals ≥ 50 years (S4a and S4b) effectively reduced hospitalizations and deaths, it under-performed when it was combined with a school closure. Amongst all scenarios, S6g (a 5-month stay-at-home order for individuals ≥ 50 years and a 4-month school closure) performed

the poorest, with over 40.7% (IQR: 38.5% to 43.5%) increase in hospitalizations and 54.7% (IQR: 51.8% to 57.7%) increase in deaths per 10,000 population, as compared to scenario S4b (a 5-month stay-at-home order for individuals aged 50 and older).

6.8 Impact of scenarios

In general, all strategies reduced the number of infections, hospitalizations, and deaths at the outbreak peak as compared to the baseline scenario (S0). With self-isolation of 20% mild and 100% severe cases, a 26.1% (IQR: 24.9% to 27.3%) reduction in total infections was observed, along with at least 81% reduction in hospitalized cases and deaths. Clearly, S1 was not the optimal scenario as disease burden could be further reduced with the inclusion of other stay-at-home orders. The lockdown scenario (S2) reduced disease incidence significantly, especially during the lockdown period as compared to S1. However, a complete lockdown has two major drawbacks: (i) 100% of the population must practice stay-at-home order, which would impact the socioeconomic well-being of the population, and (ii) the sudden rise in disease incidence after the lockdown period ended if the disease not eliminated. Figure 6.11 shows that although S2 effectively reduced infections, it under-performed in reducing hospitalizations and deaths as compared to S3 and S4.

For a 3-month or 5-month stay-at-home order that targeted individuals aged 65 and older (S3), the reduction of hospitalizations was 17.9% (IQR: 16.4% to 19.5%) and 29.1% (IQR: 27.8% to 30.2%), respectively. A 3-month and 5-month stay-at-home order that targeted individuals aged 50 and older further increased the reduction of hospitalizations to 28.5% (IQR: 27.0% to 29.7%) and 47.5% (IQR: 46.5% to 48.4%), respectively. For stay-at-home orders that targeted younger individuals ($5-19$ years old), only an 8-month school closure (S5d) had somewhat comparable results to S3a, with 20.7% (IQR: 19.0% to 22.2%) reduction of hospitalizations as seen in figure 6.7. These results indicated that S4 out-performed other strategies, with 34.2% (IQR: 33.0% to 35.4%) and 55.0% (IQR: 54.1% to 56.0%) reduction of deaths for 3 months and 5 months stay-at-home orders, respectively, as compared to S1. The second highest reduction in deaths was observed in stay-at-home orders that targeted individuals aged 65 and older (17% of the population), with 30.7%

(IQR: 29.3% to 31.9%) and 48.5% (IQR: 47.3% to 49.2%) reduction of deaths for 3 months (S3a) and 5 months (S3b) stay-at-home order, respectively. In terms of reducing deaths, school closure was not as effective because even an 8 month school closure (S5d) only resulted in 21.2% (IQR: 19.4% to 22.9%) reduction in deaths (seen in figure 6.7), which was significantly lower than what was achieved in strategies S3 and S4. Furthermore, section 6.7 explained that S4 out-performed S6 in terms of reducing infections, hospitalizations, and deaths. Overall, it is evident that S3 and S4 are most effective strategies for reducing hospitalizations and deaths and target a lower proportion of the population for stay-at-home order as compared to lockdown scenarios.

6.9 Efficiency of scenarios

The strategy efficiency (for S2-S5) was analyzed based on the number of infections, hospitalizations, and deaths averted per-person practicing the stay-at-home order. For a 3-month or 5-month stay-at-home order, S4 (in which 37% of the population practising the stay-at-home order) was efficient in reducing infections, while S3 (in which 17% of the population practising the stay-at-home order) was efficient in reducing hospitalizations and deaths. Specifically, for a 3-month stay-at-home order, S4a had 0.14 (IQR: 0.12 to 0.16) infections averted per person, and S3a had 0.0053 (IQR: 0.0048 to 0.0058) hospitalizations and 0.0017 deaths (IQR: 0.0016 to 0.0018) averted per-person. Extending the stay-at-home order to 5 months showed similar results, with S4b having 0.26 (IQR: 0.24 to 0.28) infections averted per person, and S3b leading to 0.0087 (IQR: 0.0082 to 0.0092) hospitalizations and 0.0027 (IQR: 0.0026 to 0.0028) deaths averted per-person. In comparison with other scenarios, S5a and S5b were the least efficient even though they have the same proportion of individuals practising the stay-at-home order as S3a and S3b. We explicate that the variation in strategy efficiency for S3 and S5 is due to the dynamics of age-groups that are targeted for the stay-at-home order. For instance, S5 targets individuals in age-group $5 - 19$ years who have less hospitalizations and deaths compared to individuals in age-group ≥ 65 years in S3. Overall, stay-at-home orders that target older age-groups (individuals ≥ 50 years) have the highest strategy efficiency. Although a longer duration of school closure (S5c and S5d) showed the highest number of infections averted

per-person, it had lower hospitalization and deaths averted per-person as compared to S3 and S4. S2 was the least efficient as it had the lowest number of infections, hospitalizations, and deaths averted per-person practising the stay-at-home order.

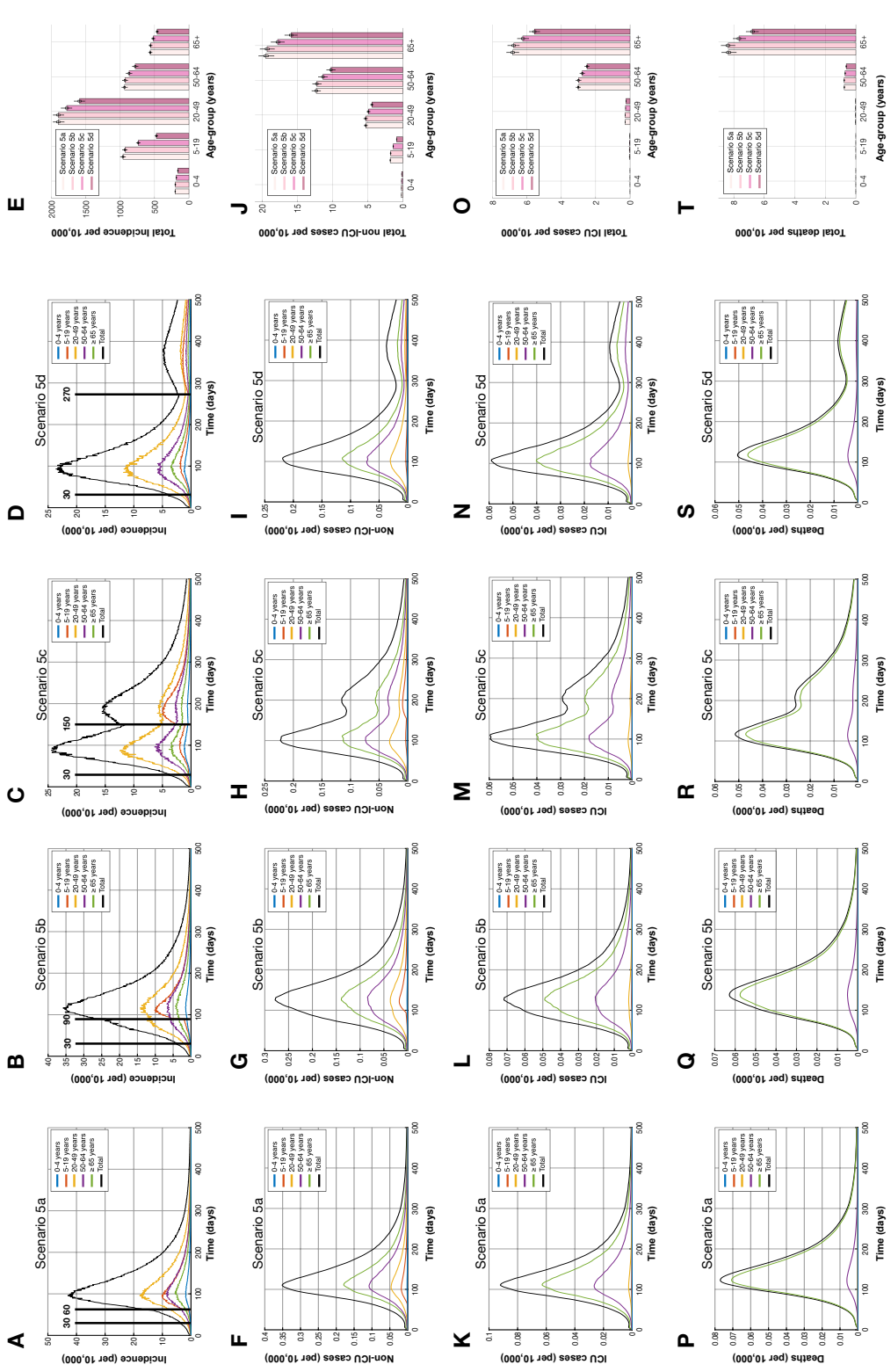

Figure 6.6: The average projected curves for daily incidence, non-ICU cases, ICU cases, and deaths for: (i) S5a are shown in A,F,K,P, (ii) S5b are shown in B,G,L,Q, (iii) S5c are shown in C,H,M,R, and (iv) S5d are shown in D,I,N,S, respectively. The vertical bars in A,B,C, and D show the start and end of the stay-at-home order for each scenario. The cumulative incidence (E), non-ICU cases (J), ICU cases (O), and deaths (T) are shown for S5a,S5b,S5c, and S5d. For graphs E,J,O, and T, the bars show the mean values and the boxplots show the median and IQR values. These estimates and projections are per 10,000 population.

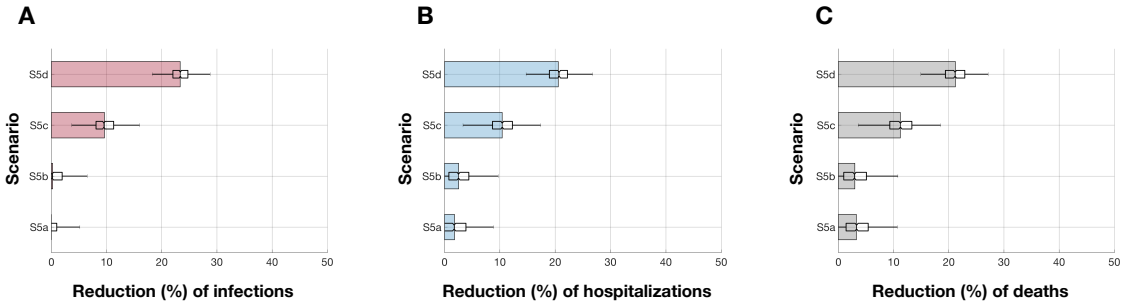

Figure 6.7: A,B, and C are the reduction in cumulative infections, cumulative hospitalizations, and cumulative deaths compared to S1 (self isolation for 20% mild cases and 100% severe cases). The bars show the mean values and the boxplots show the median and IQR values.

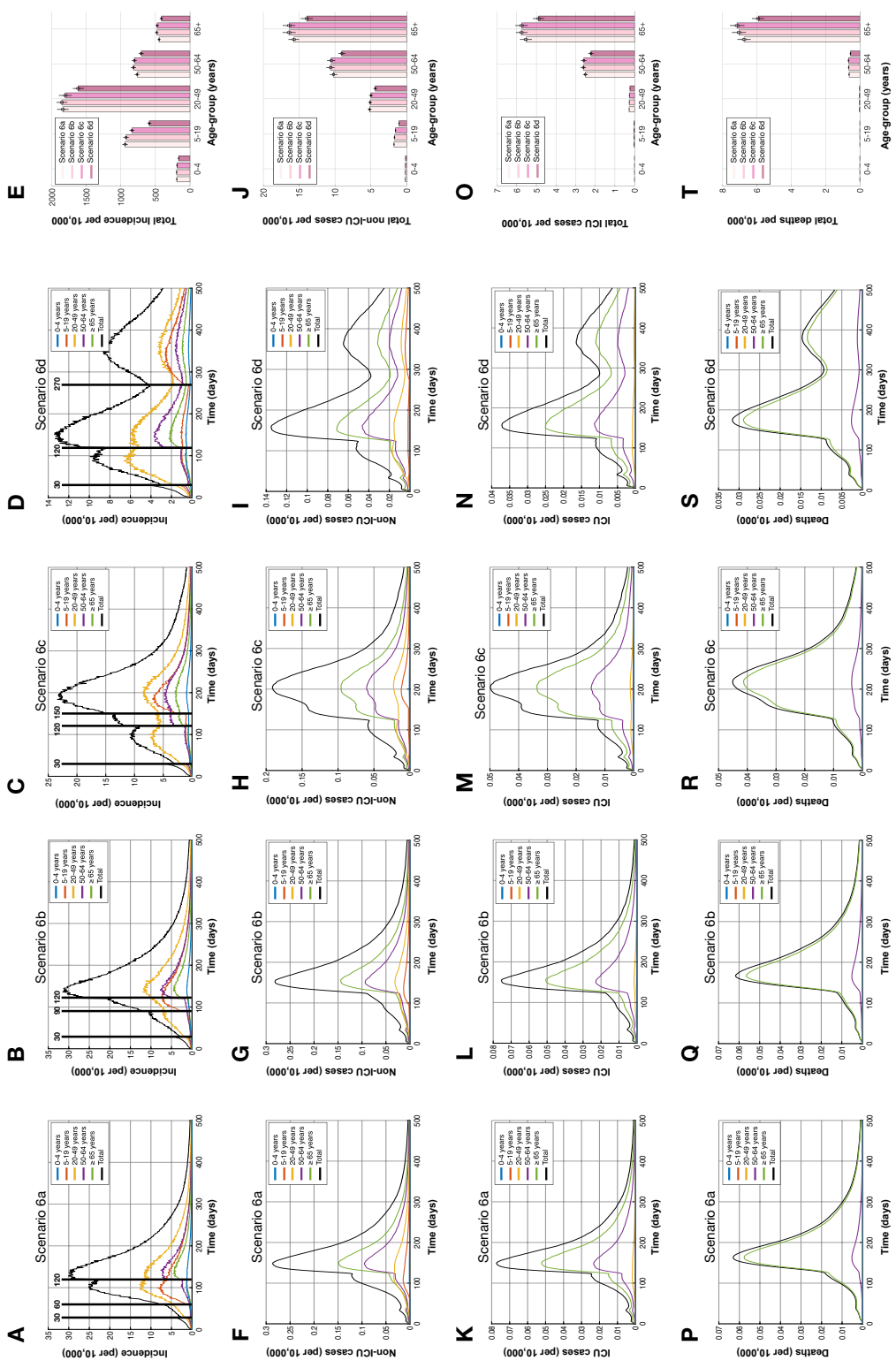

Figure 6.8: The average projected curves for daily incidence, non-ICU cases, ICU cases, and deaths for: (i) S6a are shown in A,F,K,P, (ii) S6b are shown in B,G,L,Q, (iii) S6c are shown in C,H,M,R, and (iv) S6d are shown in D,I,N,S, respectively. The vertical bars in A,B,C, and D show the start and end of the stay-at-home order for each scenario. The cumulative incidence (E), non-ICU cases (J), ICU cases (O), and deaths (T) are shown for S6a,S6b,S6c, and S6d. For graphs E,J,O, and T, the bars show the mean values and the boxplots show the median and IQR values. These estimates and projections are per 10,000 population.

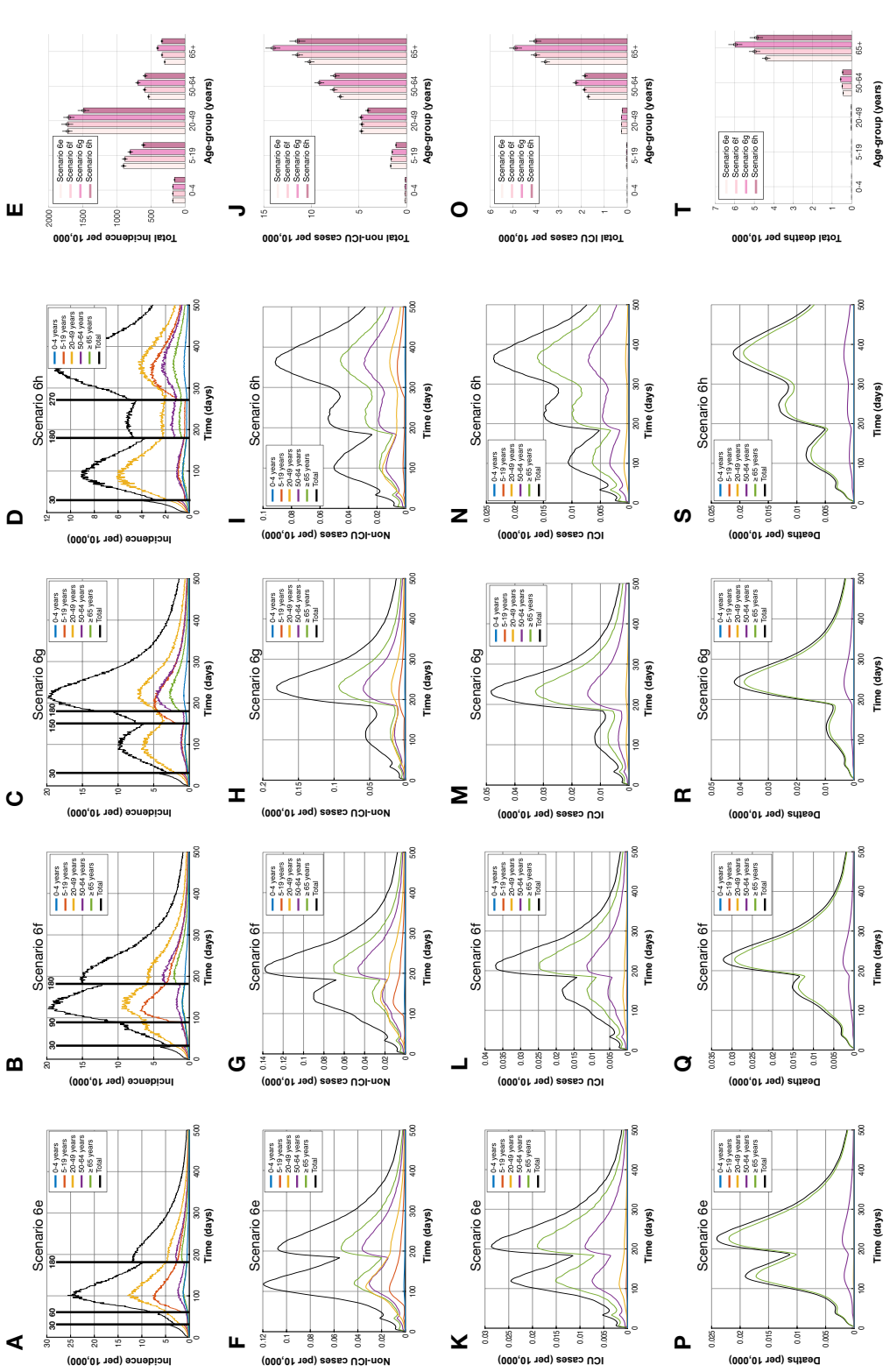

Figure 6.9: The average projected curves for daily incidence, non-ICU cases, ICU cases, and deaths for: (i) S6e are shown in A,F,K,P, (ii) S6f are shown in B,G,L,Q, (iii) S6g are shown in C,H,M,R, and (iv) S6h are shown in D,I,N,S, respectively. The vertical bars in A,B,C, and D show the start and end of the stay-at-home order for each scenario. The cumulative incidence (E), non-ICU cases (J), ICU cases (O), and deaths (T) are shown for S6e,S6f,S6g, and S6h. For graphs E,J,O, and T, the bars show the mean values and the boxplots show the median and IQR values. These estimates and projections are per 10,000 population.

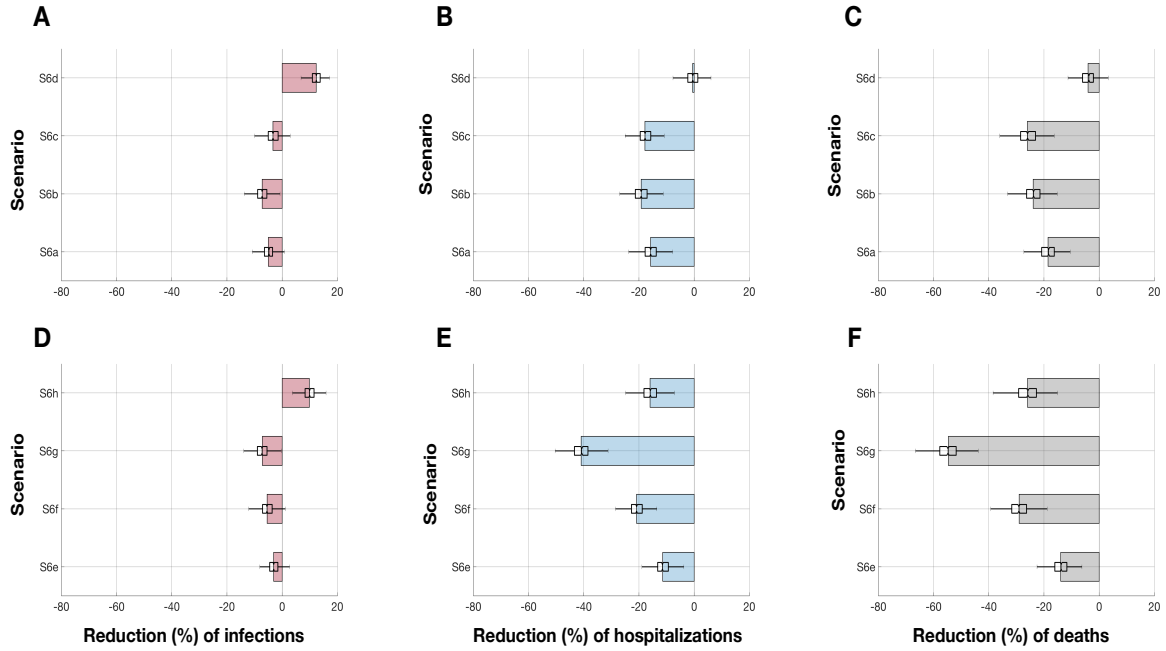

Figure 6.10: Graphs A,B, and C are the percent reduction in infections, hospitalizations, and deaths compared to S4a (3 month stay-at-home order for individuals ≥ 50). Graphs D, E, and F are the percent reduction in infections, hospitalizations, and deaths compared to S4b (5 month stay-at-home order for individuals ≥ 50 years). The bars show the mean values and the boxplots show the median and IQR values.

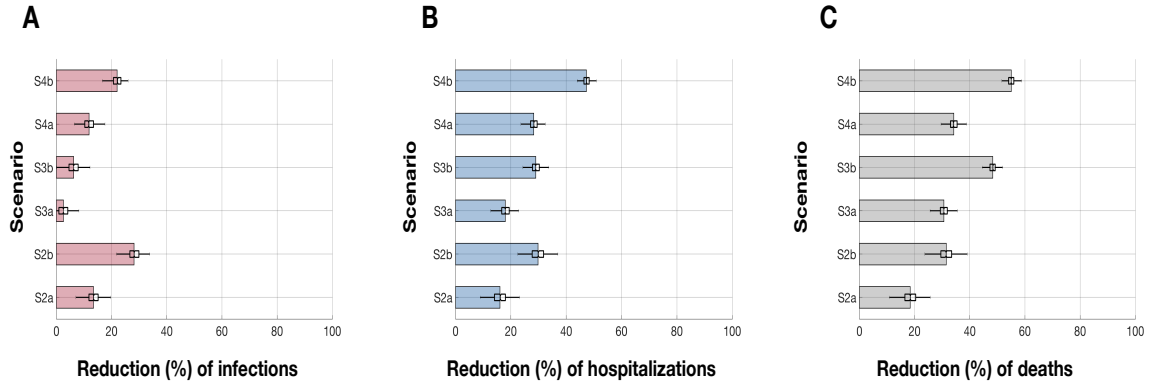

Figure 6.11: A,B, and C are the percent reduction in infections, hospitalizations, and deaths compared to S1 (self-isolation of 20% mild cases and 100% severe cases). The bars show the mean values and the boxplots show the median and IQR values.

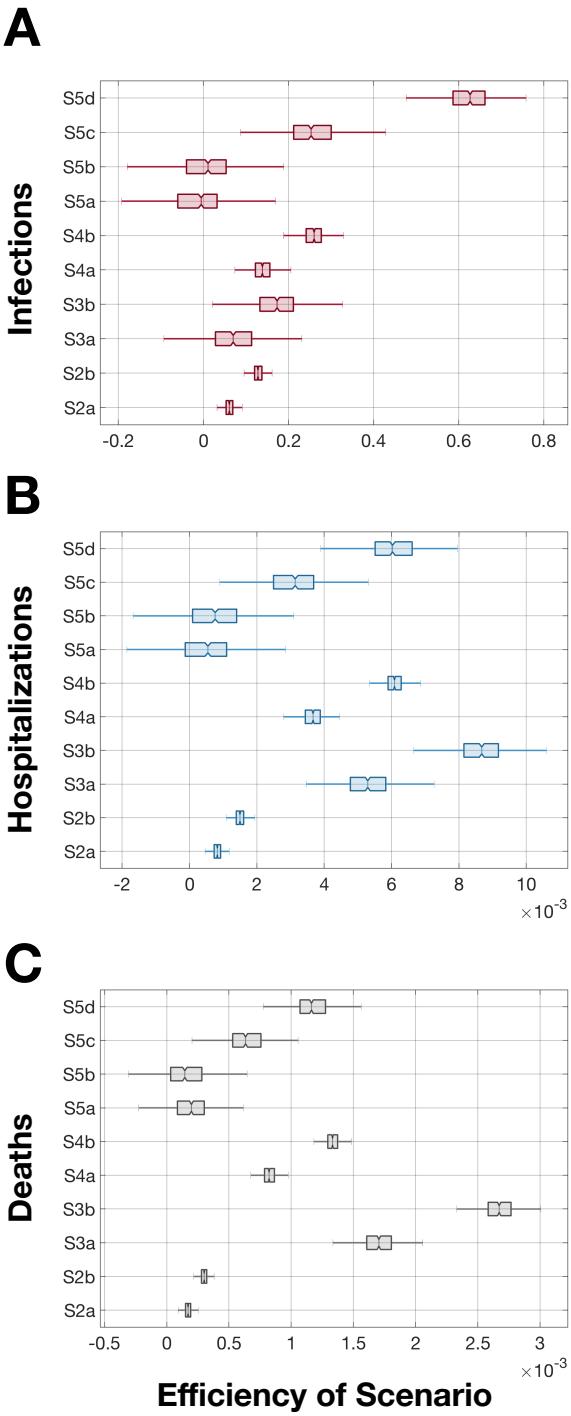

Figure 6.12: A,B, and C show the efficiency of the scenarios. Scenario efficiency is the number of infections (A), hospitalizations (B), and deaths (C) averted per person practising the stay-at-home order.

Chapter 7

Discussion

The COVID-19 pandemic continues to be an ongoing major public health challenge that has caused enormous strain on healthcare systems around the world. During the initial stages of the pandemic, public health officials resorted to traditional methods, such as social distancing and stay-at-home orders (i.e., lockdowns), to limit disease spread and reduce the hospitalizations and deaths. Although these interventions reduced human-to-human interactions, they had a negative impact on socioeconomic aspects of life in many countries due to closure of major businesses and activities. A key question that remained unanswered at the time was the optimality of these measures at controlling disease spread. This thesis aimed to identify the impact of different age-specific stay-at-home orders on infections, hospitalizations, and deaths. This work is useful in identifying effective and efficient strategies for COVID-19 disease management post-lockdown and other emerging infectious diseases.

The results of this thesis showed that although the lockdown scenario (S2) was effective at delaying and reducing the peak of incidence, it under-performed scenario S3 (stay-at-home order for ≥ 65 years) and S4 (stay-at-home order for ≥ 50 years) in reducing hospitalizations and deaths. In fact, a stay-at-home order for individuals ≥ 65 years (S3) projected to be the most efficient strategy in reducing hospitalizations and deaths, which did not affect the majority of the working population (individuals $20 - 49$ years). This would ensure that a significant proportion of the population may continue to work and thereby eliminating some of the economic consequences

that arise due to a complete lockdown. For strategies that target older age-groups, S4 (37% of the population) under-performed S3 (17% of the population), particularly with regards to the number of hospitalizations and deaths averted per-person. Not only did S3 have a smaller proportion of population practising the stay-at-home order, but also it targeted the age-group with the highest hospitalization and death rates. Although school closure also targeted 17% (the same proportion as S3) of the population, it under-performed in reducing hospitalizations and deaths. This suggests that strategies targeting younger age-groups for stay-at-home orders were not as effective as strategies targeting older age-groups because younger individuals mostly interacted amongst themselves and were less likely to develop severe symptoms or require hospitalization. Notably, school closure (S5) implemented for a longer duration, such as 4 or 8 months, reduced the peak of incidence; however, the reduction in hospitalizations and deaths was less compared to strategies targeting individuals ≥ 50 years (S3 and S4). Therefore, a school closure strategy may only be useful in managing a short-term surge in infections by reducing peak incidence; however, it will not be effective at reducing the burden on healthcare systems. As additional analysis, S4 was combined with school closure (S5) to determine if this would result in a further reduction in the outcomes of interest. Surprisingly, the results showed an increase in infections, hospitalizations, and deaths compared to S4, perhaps due to the emergence of second or third waves that arose after the stay-at-home orders were lifted. This indicates that increasing the proportion of individuals practising the stay-at-home order from 37% (S4) to 54% (S6) does not necessarily result in a further reduction in the outcomes of interest. This may in part be explained by factors such as, the mixing patterns amongst individuals targeted for stay-at-home orders and the timing and duration of interventions. In general, strategically implementing age-specific stay-at-home orders is important for minimizing disease incidence.

Models are great tools for predicting potential outcomes of important public health decisions; however, these outcomes are highly dependent on the assumptions made during the development of the model. The modelling work in this thesis is deterministic in nature, therefore the results of this thesis should be taken with consideration of model assumptions and stochastic projections, which account for random events. For instance, the model does not consider any

infection transmission in the hospital because it is assumed that hospitalized individuals were perfectly isolated and the staff were following strict infection control measures (i.e., use of personal protective equipment, sanitizing routines). This assumption is based on community transmission being the major driver of disease spread rather than hospital transmission [49]. However, there have been 114 hospital outbreaks in Ontario as of October 17, 2020 [50], which implies that this assumption may need to be revised in future modelling efforts. The model also considered only two disease control measures (i.e., self-isolation of infected individuals and stay-at-home orders), which mainly focus on reducing human-to-human interactions. This is a reasonable assumption, because disease spread only occurred through direct interactions between susceptible and infectious individuals. Future modeling work should also incorporate workplaces and interactions in different locations to identify their contributions to disease incidence. Furthermore, extension of this work would be important to identify the optimal timing and duration of control measures to minimize the burden of disease. Finally, as new information and data becomes available, more accurate estimates of parameter values and distributions can be found. Thus, this modeling framework can be used to reproduce and update quantitative results based on emerging evidence.

With the availability of COVID-19 vaccine (e.g., Pfizer-BioNTech and Moderna) [51], the model presented here can also be extended to include vaccination and address critical public health questions. Some of the questions that can be answered with the inclusion of vaccination dynamics are: (i) Which stay-at-home strategy (analyzed in this thesis) would be effective to use during the implementation of mass-vaccination campaigns? (ii) Is it safe to lift stay-at-home orders if a proportion of population on the priority list or high-risk groups have been vaccinated?, (iii) Which age-groups should be on the priority list?, (iv) If there is a shortage of supply, what is the optimal vaccine allocation (for each age-group) within the population?, and (v) what percentage of people on the priority list should be vaccinated before the general public can receive vaccines?. The answers to these questions can help guide and optimize the COVID-19 vaccination campaigns and aid the safe re-opening of the community. Additionally, with the recent emergence of highly transmissible SARS-CoV-2 variants [52–54], this model can be extended to include the possibility of re-infection (i.e., due to a potential vaccine resistant COVID-19 variant) or a vaccine resistant

class. This can be used to predict the impact of future vaccine resistant strains and provide useful information to healthcare systems so they can prepare and plan for potential challenges.

This thesis has important implications for stay-at-home orders for COVID-19 and other emerging infectious diseases. A complete lockdown is effective in immediately reducing peak incidence; however it is important to strategically lift lockdown orders by using age-specific stay-at-home orders. Although the feasibility of stay-at-home orders is an area for further research, this work suggests that hospitalizations and deaths are minimized when older individuals (≥ 50 years) are advised to stay-at-home. Due to the emergence of additional waves, this strategic response combined with vaccine campaigns will be important for minimizing the burden on healthcare systems until herd immunity is reached (by vaccinating individuals).

Bibliography

1. Anderson, R. M. & May, R. M. The population dynamics of microparasites and their invertebrate hosts. *Philosophical Transactions of the Royal Society of London. B, Biological Sciences* **291,** 451–524 (1981).

2. Roddam, A. W. *Mathematical Epidemiology of Infectious Diseases: Model Building, Analysis and Interpretation: O Diekmann and JAP Heesterbeek, 2000, Chichester: John Wiley pp. 303,£ 39.95. ISBN 0-471-49241-8* 2001.

3. Mollison, D. & Denis, M. *Epidemic models: their structure and relation to data* (Cambridge University Press, 1995).

4. WHO. *Listings of WHO's response to COVID-19* June 2020. https://www.who.int/news/item/29-06-2020-covidtimeline.

5. Centers for Disease Control and Prevention. *Symptoms of Coronavirus* Sept. 2020. https://www.cdc.gov/coronavirus/2019-ncov/symptoms-testing/symptoms.html.

6. Centers for Disease Control and Prevention. People at Increased Risk And Other People Who Need to Take Extra Precautions. *Coronavirus Disease 2019 (COVID-19).* https://www.cdc.gov/coronavirus/2019-ncov/need-extra-precautions/index.html (Sept. 2020).

7. McCann, A., Popovich, N. & Wu, J. Italy's Virus Shutdown Came Too Late. What Happens Now? *The New York Times.* https://www.nytimes.com/interactive/2020/

04/05/world/europe/italy-coronavirus-lockdown-reopen.html (Apr. 2020).

8. The Canadian Press. Timeline of COVID-19 cases across Canada. *CBC NEWS*. https://www.cbc.ca/news/health/canada-coronavirus-timeline-1.5482310 (Mar. 2020).

9. Sandford, A. & Euronews. Coronavirus: Half of humanity now on lockdown as 90 countries call for confinement. *Euronews*. https://www.euronews.com/2020/04/02/coronavirus-in-europe-spain-s-death-toll-hits-10-000-after-record-950-new-deaths-in-24-hou (Apr. 2020).

10. Li, Q. *et al.* Early transmission dynamics in Wuhan, China, of novel coronavirus–infected pneumonia. *New England Journal of Medicine* (2020).

11. Muccari, R., Chow, D. & Murphy, J. *Coronavirus timeline: Tracking the critical moments of COVID-19* July 2020. https://www.nbcnews.com/health/health-news/coronavirus-timeline-tracking-critical-moments-covid-19-n1154341.

12. Kinetz, E. *Where did they go? Millions left Wuhan before quarantine* Feb. 2020. https://www.ctvnews.ca/health/where-did-they-go-millions-left-wuhan-before-quarantine-1.4803739.

13. The New York Times. Coronavirus Death Toll Climbs in China, and a Lockdown Widens. *The New York Times*. https://www.nytimes.com/2020/01/23/world/asia/china-coronavirus.html (Mar. 2020).

14. Dunford, D. *et al.* Coronavirus: The world in lockdown in maps and charts. *BBC NEWS*. https://www.bbc.com/news/world-52103747 (Apr. 2020).

15. Dong, E., Du, H. & Gardner, L. An interactive web-based dashboard to track COVID-19 in real time. *The Lancet infectious diseases* **20,** 533–534 (2020).

16. Jones, A. M. WHO warns countries could see 'immediate second peak' if restrictions lifted too early. *CTV NEWS.* https://www.ctvnews.ca/health/coronavirus/who-warns-countries-could-see-immediate-second-peak-if-restrictions-lifted-too-early-1.4954512 (May 2020).

17. Johns Hopkins Medicine. *First and Second Waves of Coronavirus* Aug. 2020. https://www.hopkinsmedicine.org/health/conditions-and-diseases/coronavirus/first-and-second-waves-of-coronavirus.

18. Vogel, L. COVID-19: A timeline of Canada's first-wave response. *CMAJ News* (2020).

19. Crawley, M. Ontario's 2nd wave of COVID-19 forecast to peak in October. *CBC NEWS.* https://www.cbc.ca/news/canada/toronto/ontario-covid-19-second-wave-cases-modelling-projections-1.5739411 (Sept. 2020).

20. Government of Ontario. *COVID-19 case data: All Ontario* https://covid-19.ontario.ca/data.

21. Ferretti, L. *et al.* Quantifying SARS-CoV-2 transmission suggests epidemic control with digital contact tracing. *Science* **368** (2020).

22. He, X. *et al.* Temporal dynamics in viral shedding and transmissibility of COVID-19. *Nature medicine* **26,** 672–675 (2020).

23. Moghadas, S. M. *et al.* The implications of silent transmission for the control of COVID-19 outbreaks. *Proceedings of the National Academy of Sciences* **117,** 17513–17515 (2020).

24. Lauer, S. A. *et al.* The incubation period of coronavirus disease 2019 (COVID-19) from publicly reported confirmed cases: estimation and application. *Annals of internal medicine* **172,** 577–582 (2020).

25. Qin, J. *et al.* Estimation of incubation period distribution of COVID-19 using disease onset forward time: a novel cross-sectional and forward follow-up study. *medRxiv* (2020).

26. Mizumoto, K., Kagaya, K., Zarebski, A. & Chowell, G. Estimating the asymptomatic proportion of coronavirus disease 2019 (COVID-19) cases on board the Diamond Princess cruise ship, Yokohama, Japan, 2020. *Eurosurveillance* **25,** 2000180 (2020).

27. Nishiura, H. *et al.* Estimation of the asymptomatic ratio of novel coronavirus infections (COVID-19). *International journal of infectious diseases* **94,** 154 (2020).

28. Moghadas, S. M. *et al.* Projecting hospital utilization during the COVID-19 outbreaks in the United States. *Proceedings of the National Academy of Sciences* **117,** 9122–9126 (2020).

29. Wells, C. R. *et al.* Projecting the demand for ventilators at the peak of the COVID-19 outbreak in the USA. *The Lancet Infectious Diseases* (2020).

30. Zhang, K., Vilches, T. N., Tariq, M., Galvani, A. P. & Moghadas, S. M. The impact of mask-wearing and shelter-in-place on COVID-19 outbreaks in the United States. *International Journal of Infectious Diseases* (2020).

31. Heffernan, J. M., Smith, R. J. & Wahl, L. M. Perspectives on the basic reproductive ratio. *Journal of the Royal Society Interface* **2,** 281–293 (2005).

32. Van den Driessche, P. & Watmough, J. Reproduction numbers and sub-threshold endemic equilibria for compartmental models of disease transmission. *Mathematical biosciences* **180,** 29–48 (2002).

33. Van den Driessche, P. Reproduction numbers of infectious disease models. *Infectious Disease Modelling* **2,** 288–303 (2017).

34. Weisstein, E. W. Characteristic polynomial. *https://mathworld. wolfram. com/* (2002).

35. Randolph, H. E. & Barreiro, L. B. Herd Immunity: Understanding COVID-19. *Immunity* **52,** 737–741 (2020).

36. Britton, T., Ball, F. & Trapman, P. A mathematical model reveals the influence of population heterogeneity on herd immunity to SARS-CoV-2. *Science* **369,** 846–849 (2020).

37. Gomes, M. G. M. *et al.* Individual variation in susceptibility or exposure to SARS-CoV-2 lowers the herd immunity threshold. *medRxiv* (2020).

38. Chung, E. & Zafar, A. *Once someone is vaccinated, do they still have to wear a mask? Your COVID-19 vaccine questions answered | CBC News* Dec. 2020. `https://www.cbc.ca/news/health/covid-19-general-vaccine-faq-1.5838140`.

39. Aschwanden, C. The false promise of herd immunity for COVID-19. *Nature* (2020).

40. Gatto, M. *et al.* Spread and dynamics of the COVID-19 epidemic in Italy: Effects of emergency containment measures. *Proceedings of the National Academy of Sciences* **117,** 10484–10491 (2020).

41. Li, R. *et al.* Substantial undocumented infection facilitates the rapid dissemination of novel coronavirus (SARS-CoV-2). *Science* **368,** 489–493 (2020).

42. Shoukat, A. *et al.* Projecting demand for critical care beds during COVID-19 outbreaks in Canada. *CMAJ* **192,** E489–E496 (2020).

43. Sanche, S. *et al.* The novel coronavirus, 2019-nCoV, is highly contagious and more infectious than initially estimated. *arXiv preprint arXiv:2002.03268* (2020).

44. Yang, X. *et al.* Clinical course and outcomes of critically ill patients with SARS-CoV-2 pneumonia in Wuhan, China: a single-centered, retrospective, observational study. *The Lancet Respiratory Medicine* (2020).

45. Wu, J. T., Leung, K. & Leung, G. M. Nowcasting and forecasting the potential domestic and international spread of the 2019-nCoV outbreak originating in Wuhan, China: a modelling study. *The Lancet* **395,** 689–697 (2020).

46. Mossong, J. *et al.* Social contacts and mixing patterns relevant to the spread of infectious diseases. *PLoS Med* **5,** e74 (2008).

47. Jarvis, C. I. *et al.* Quantifying the impact of physical distance measures on the transmission of COVID-19 in the UK. *BMC medicine* **18,** 1–10 (2020).

48. Moghadas, S. M. & Jaberi-Douraki, M. *Mathematical Modelling: A Graduate Textbook* (John Wiley & Sons, 2018).

49. Crawley, M. People are getting COVID-19 by community transmission, but Ontario knows little about how. *CBC NEWS*. https://www.cbc.ca/news/canada/toronto/contracting-covid19-ontario-1.5548087 (Apr. 2020).

50. Ontario Agency for Health Protection and Promotion (Public Health Ontario). *Epidemiologic summary: COVID-19 in Ontario – January 15, 2020 to October 23, 2020* Oct. 2020. https://www.publichealthontario.ca/-/media/documents/ncov/epi/2020/covid-19-daily-epi-summary-report.pdf?la=en.

51. Government of Ontario. https://covid-19.ontario.ca/covid-19-vaccines-ontario.

52. Philip, E., Favaro, A. & Jones, A. New variants of novel coronavirus detected worldwide, worrying public health experts. *Coronavirus News*. https://www.ctvnews.ca/health/coronavirus/new-variants-of-novel-coronavirus-detected-worldwide-worrying-public-health-experts-1.5274052 (Jan. 2021).

53. Reuters, T. *Japan identifies new virus variant as global COVID-19 tally tops 90 million | CBC News* Jan. 2021. https://www.cbc.ca/news/canada/coronavirus-covid19-canada-world-january-10-2021-1.5867773.

54. Fox, C. *Ontario officials concerned about community spread of UK COVID-19 variant as 8 more cases are confirmed* Jan. 2021. https://toronto.ctvnews.ca/ontario-officials-concerned-about-community-spread-of-uk-covid-19-variant-as-8-more-cases-are-confirmed-1.5263663.